https://doi.org/10.5194/esd-2024-24
Preprint. Discussion started: 22 August 2024

Earth System Dynamics Discussions
Open Access
EGU

Impact of Greenland Ice Sheet Disintegration on Atmosphere and Ocean Disentangled

Malena Andernach[1,2], Marie-Luise Kapsch[1], and Uwe Mikolajewicz[1]

[1]Max Planck Institute for Meteorology, Hamburg, Germany
[2]International Max Planck Research School for Earth System Modelling (IMPRS), Hamburg, Germany

Correspondence: Malena Andernach (malena.andernach@mpimet.mpg.de)

Abstract. We analyze the impact of a disintegrated Greenland Ice Sheet (GrIS) on the global climate through steady-state simulations with the MPI-ESM (Max Planck Institute for Meteorology Earth System Model). This advances our understanding of the intricate feedbacks between the GrIS and the full climate system. Sensitivity experiments enable the quantification of the individual contributions of altered Greenland surface elevation and properties (e.g., land cover) to the atmospheric and oceanic climate response. Removing the GrIS results in reduced mechanical atmospheric blocking, warmer air temperatures over Greenland and thereby changes in the atmospheric circulation. The latter alters the wind stress on the ocean, which controls the ocean-mass transport through the Arctic Gateways. Without the GrIS, the upper Nordic Seas are fresher, attenuating deep-water formation. In the Labrador Sea, deep-water formation is weaker despite a higher upper-ocean salinity, as the inflow of dense overflow from the Denmark Strait is reduced. Our sensitivity experiments show that the atmospheric response is primarily driven by the lower surface elevation, whereas altered Greenland surface properties mostly amplify but also counteract few of the changes. The lower Greenland elevation dominates the ocean response through wind-stress changes. Only in the Labrador Sea, altered Greenland surface properties dominate the ocean response, as this region stores excessive heat from the Greenland warming. The main drivers vary vertically: The elevation effect controls upper-ocean densities, while surface properties are important for the intermediate and deep ocean. Despite the confinement of most responses to the Arctic, a disintegrated GrIS also influences remote climates. The altered climate in response to a GrIS disintegration also constrains a potential ice-sheet regrowth to high-bedrock eastern Greenland.

1 Introduction

Located between 60 and 85° N and characterized by steep topography with peaks exceeding 3,000 m, the Greenland Ice Sheet (GrIS) is a prominent feature in the Northern Hemisphere that not only impacts the local climate (Box et al., 2012; Oerlemans and Vugts, 1993; van den Broeke et al., 1994), but also the remote climate (Lunt et al., 2004; Davini et al., 2015). In view of the present mass loss (Shepherd et al., 2020) and potential disappearance of the GrIS under ongoing anthropogenic global warming (Aschwanden et al., 2019), the interplay between GrIS characteristics and the broader climate system is imperative to understand. A number of studies have investigated potential climatic effects of a completely or almost completely melted GrIS on the Northern Hemisphere Earth system under various climates (e.g., Crowley et al., 1994; Crowley and Baum, 1995;

https://doi.org/10.5194/esd-2024-24
Preprint. Discussion started: 22 August 2024


Earth System Dynamics Discussions Open Access EGU

Davini et al., 2015; Toniazzo et al., 2004; Lunt et al., 2004; Hakuba et al., 2012; Junge et al., 2005; Vizcaíno et al., 2008; Petersen et al., 2004; Dethloff et al., 2004; Kristjánsson and Mcinnes, 1999; Kristjánsson et al., 2009; Ridley et al., 2005; Solgaard and Langen, 2012; Stone and Lunt, 2013; Merz et al., 2014a, b). These studies found considerable climatic changes, both thermodynamic and dynamic, in response to a reduced GrIS volume. However, a clear separation between the two primary effects of a disintegrated GrIS - lower surface elevation and altered surface properties (e.g., land cover) - and their respective contributions to the changed climate has yet to be established. The primary objective of the present study is to systematically analyse the interactions of the GrIS with the atmosphere and ocean, whereby we specifically focus on ocean dynamics.

Disentangling the impact of the two aforementioned effects on the atmosphere and ocean remained yet challenging, as 1) coupled atmosphere-ocean models with interactive ice sheets (Ridley et al., 2005; Vizcaíno et al., 2008) require the inclusion of a myriad of feedback mechanisms that complicate the attribution of simulated climate changes to specific processes and 2) ocean models require a long-enough model spin-up to equilibrate the deep ocean, which is computationally demanding. Hence, most previous studies restricted their analysis of the impact of modified GrIS surface elevation and surface properties on the climate system to the interaction with the atmosphere, using prescribed sea-surface temperature (SST) and sea-ice conditions (Crowley et al., 1994; Crowley and Baum, 1995; Dethloff et al., 2004; Hakuba et al., 2012; Junge et al., 2005; Kristjánsson and Mcinnes, 1999; Kristjánsson et al., 2009; Merz et al., 2014a, b; Petersen et al., 2004), or they only considered the response of the upper ocean by using a simplified ocean model (Lunt et al., 2004). Few studies also highlighted the importance of the GrIS surface elevation and properties under either pre-industrial (PI) or present-day conditions for the ocean system without using external freshwater forcing. Although these studies used a dynamic ocean component within a coupled Atmosphere–Ocean General Circulation Model (AOGCM) (Davini et al., 2015; Toniazzo et al., 2004), their analyses did not consider a long-enough model spin-up compared to the time scales of the deep ocean. This constrains the exploration of interactions and feedbacks with the deep ocean. In addition to these limitations, the aforementioned studies lack a differentiation between the individual contributions of GrIS surface elevation and properties on the climate changes. Only Stone and Lunt (2013) conducted additional sensitivity experiments to separate between the two effects using a coupled AOGCM. However, their study is constrained to the analysis of atmospheric feedbacks. Similarly, Lunt et al. (2004) limited their analysis of individual contributions to air temperature differences. Lastly, most of the aforementioned studies focused on the climate impacts of a disintegrated GrIS on Greenland and the adjacent regions. Here, we extend those studies by examining the interactions of the GrIS with the entire climate system, including the deep ocean, which is imperative, particularly in light of the recent accelerated mass loss of the GrIS under global warming. Further, we point towards the remote effects of a disintegrated GrIS, e.g., the impact on European temperatures.

To study the global climate response to a complete disintegration of the GrIS, we conducted a set of steady-state coupled atmosphere-ocean-dynamic-vegetation simulations, using the Max Planck Institute for Meteorology Earth System Model (MPI-ESM) with fixed ice sheets. We disentangle the individual contributions of the reduced GrIS surface elevation and altered surface properties, by changing the GrIS height and extent as well as land cover between simulations. Additional sensitivity experiments allow us to separate between the feedback of the GrIS with the atmosphere and ocean. A multi-millennium spin-up until equilibrium allows for the analysis of the deep ocean. This approach enables us to complement previous studies by a

https://doi.org/10.5194/esd-2024-24
Preprint. Discussion started: 22 August 2024


Earth System Dynamics Discussions Open Access EGU

systematic attribution of the effects of a disintegrated GrIS on the full global climate system. Lastly, we investigate whether the altered climatic conditions would favor the nucleation of a new ice sheet in Greenland by running an offline energy balance model under the changed climate conditions. Understanding the factors that influence the formation and stability of a new ice sheet is crucial for comprehending the long-term implications of the observed climatic changes in response to a complete GrIS disintegration on the Earth system.

The structure of this paper is as follows: In Sect. 2, we describe the model setup and the experimental design. Section 3 presents the results, starting with the feedback mechanisms between the GrIS and the atmosphere, followed by the ocean interaction. The last part of that section answers the question whether a new ice sheet could grow under the changed climatic conditions. In Sect. 4, these findings are discussed with respect to previous findings, followed by a conclusion in Sect. 5.

2 Methods

To investigate the climate response to different states of the GrIS, we conducted a systematic set of model simulations with MPI-ESM. The first three simulations differ in terms of their GrIS extent and height as well as the retention of their glacier mask. Additional experiments serve to understand the respective effects on the atmosphere and/or ocean and the feedback between these components. Table 1 gives an overview of all experiments.

2.1 Model system

For this study, we used MPI-ESM version 1.2 in a coarse resolution (Mauritsen et al., 2019). The model consists of the ECHAM6.3 spectral atmospheric model (Stevens et al., 2013) at a T31 horizontal resolution (approximately 3.75°) and 31 vertical levels, the JSBACH3.2 land surface vegetation model (Raddatz et al., 2007) and the MPIOM1.6 primitive equation ocean model (Marsland et al., 2003; Mikolajewicz et al., 2007) with a nominal resolution of 3°. For more details on the model system, refer to Kapsch et al. (2022).

2.2 Experimental design

All seven simulations were started from a simulation of the last deglaciation with prescribed ice sheets from ICE-6G reconstructions (ICE6G_P3, Kapsch et al. 2022, Peltier et al. 2015) at year 1840. The first simulation, hereafter named CTRL, is a reference simulation that resembles a steady-state PI simulation based on ICE6G_P3. For this simulation we used the PI ice sheet with a maximum elevation of 3,096 m in the central region of Greenland (Fig. 1a). Further, PI greenhouse-gas concentrations (Köhler et al., 2017), insolation and orbital parameters (Berger and Loutre, 1991) were prescribed. In a second experiment, we removed the GrIS, and refer to this experiment as noGrIS (Fig. 1b). noGrIS has the same boundary and initial conditions as CTRL, except for the Greenland orography, which was taken from a simulation with the fully-coupled climate-ice-sheet-solid-earth model MPI-ESM-mPISM-VILMA. In this simulation, CO_2 concentrations follow the SSP5-8.5 emission scenario until the year 2,500 (Meinshausen et al., 2020). After year 2,500, CO_2 concentrations were taken from a CLIMBER simulation (Brovkin et al., 2012; Kleinen et al., 2021). This caused a complete disintegration of the GrIS under

https://doi.org/10.5194/esd-2024-24
Preprint. Discussion started: 22 August 2024

Earth System Dynamics Discussions
Open Access
EGU

peak CO_2 values in the MPI-ESM-mPISM-VILMA simulation. For noGrIS, we replaced the GrIS orography with the underlying isostatically-adjusted surface bedrock of the fully-coupled simulation at the time when the GrIS has completely melted. In noGrIS, highest mountains are found in the eastern and southern regions of Greenland, with a maximum elevation of about 1,320 m. We also removed the glacier mask (pink outline in Fig. 1a), allowing for the vegetation to dynamically regrow and surface parameters to change to those of a non-glaciated surface. While the model captures transitions in the vegetation, a comprehensive investigation of the feedbacks between changes in the vegetation and the climate system is out of the scope of this study. The impacts of all changes in the land cover and surface parameters are thus summarized as GrIS surface properties.

To disentangle the individual contributions of the reduced GrIS orography and the altered surface properties, we performed a third experiment, noGrIS_elev, for which we adjusted all the orographic changes as in noGrIS, but maintained the surface properties in their original, glaciated state, comparable to CTRL. For this, we kept the glacier mask constant. Note that in none of the experiments the freshwater associated with the removal of the GrIS was added into the ocean, following previous approaches (Davini et al., 2015; Lunt et al., 2004; Stone and Lunt, 2013). Further, land-sea mask and river runoff directions were kept constant. The three main experiments were integrated for 7,150 years. Equilibrium in the deep ocean emerges after approximately 4,150 years in our simulations.

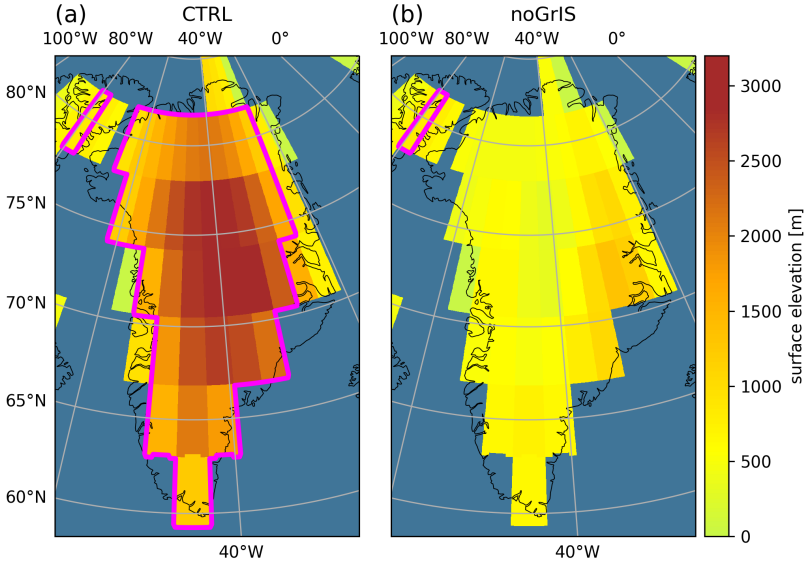

Figure 1. Surface elevation used as input to MPI-ESM for (a) CTRL and (b) noGrIS. The pink outline shows the glacier mask.

Four additional sensitivity experiments were performed to disentangle the respective impact of a disintegrated GrIS on the atmosphere and ocean. The first three experiments resemble CTRL, noGrIS and noGrIS_elev, but SST and sea-surface salinity (SSS) are nudged towards the climatology of the CTRL simulation. Hence, these experiments exclusively focus on the interaction of the GrIS with the atmosphere, suppressing the ocean response. These simulations are referred to as CTRL_atm,

https://doi.org/10.5194/esd-2024-24
Preprint. Discussion started: 22 August 2024

Earth System Dynamics Discussions
Open Access
EGU

noGrIS_atm and noGrIS_elev_atm, respectively. As the atmosphere needs less time to equilibrate than the ocean, the simulations were integrated for 3,150 years to reach a steady state.

A last experiment, referred to as CTRL_wind, was conducted to shed light on the dynamical atmospheric effects of the GrIS height reduction on the ocean. For this experiment, we maintained the same conditions as in CTRL, but applied a flux correction using the wind-stress anomaly of the simulation in which we only consider atmospheric changes in response to the elevation reduction (noGrIS_elev_atm) and CTRL_atm.

For the analysis, the final 1,000 years of each simulation were averaged and all experiments are compared to their respective control experiment. For the atmosphere, we focus our analysis on the winter season (DJF), as largest atmospheric changes in the Northern Hemisphere occur during these months. Given that the ocean responds on longer time scales than the atmosphere, our ocean and wind-stress analysis is based on annual-mean values.

Table 1. Overview of the performed experiments, including simulation length, GrIS orography (PI extent or removed GrIS), GrIS surface properties (PI or no glacier mask), or whether nudging (SST and SSS), or the application of a wind-stress anomaly flux correction from the noGrIS_elev_atm experiment was applied.

Run	Simulation length (yrs)	GrIS orography	Glacier mask	SST & SSS nudging	Prescribed wind forcing anomaly
$CTRL$	7150	PI	PI	no	no
$noGrIS$	7150	removed	removed	no	no
$noGrIS\_elev$	7150	removed	PI	no	no
$CTRL\_atm$	3150	PI	PI	yes	no
$noGrIS\_atm$	3150	removed	removed	yes	no
$noGrIS\_elev\_atm$	3150	removed	PI	yes	no
$CTRL\_wind$	7150	PI	PI	no	yes

3 Results

The implications of a disintegrated GrIS for the Earth system are analysed in the following. In Sect. 3.1, we explore the atmospheric and in Sect. 3.2 the ocean response to an absent GrIS. Section 3.4 provides a comprehensive overview of the chain of effects and contributions of the lower GrIS surface elevation and properties on the climate. Section 3.5 sheds light on the question of whether the altered climatic conditions resulting from a removal of the GrIS would be favorable for ice-sheet inception.

https://doi.org/10.5194/esd-2024-24
Preprint. Discussion started: 22 August 2024


Earth System Dynamics Discussions

3.1 Atmosphere response

The analysis of the atmospheric response to a disintegration of the GrIS is split into three parts: The first part describes the spatial and seasonal patterns of the 2 m air temperature response. The second part looks into the atmospheric processes driving the formerly described difference. The last part attributes the 2 m air temperature changes over Greenland to their respective drivers and quantifies them.

3.1.1 Near-surface air temperature response

In CTRL, the Northern Hemisphere annual-mean 2 m air temperature is 286.6 K (13.5°C), whereby Greenland experiences considerably colder conditions, with an average temperature of 254.6 K (-18.6°C, Fig. 2e). The colder conditions are a result of the unique geographical characteristics of the GrIS, including its high elevation, latitudinal position, and vast glaciated area, characterized by a highly-reflective surface.

Winter

Removing the orography of the GrIS leads to a strong warming over Greenland: The spatially averaged winter 2 m air temperature over Greenland is +7.9 K warmer in noGrIS than in CTRL, with a local maximum of +16.0 K (Fig. 2a). Across the Arctic region, a pronounced dipole pattern emerges in the winter 2 m air-temperature difference. Specifically, warmer temperatures are depicted in the western Arctic in noGrIS compared to CTRL, with a maximum across Greenland. In the remaining western Arctic, strongest differences ($\approx$ +5.0 K) occur over the Nares Strait and the Canadian Arctic Archipelago, whereas the difference is weaker over the Labrador Sea ($\approx$ +1.0 K). In contrast, the eastern Arctic experiences up to -6.0 K colder conditions in noGrIS than in CTRL, particularly over the Nordic Seas, the Barents Sea and northern Europe. This dipole pattern is also reflected in the SST and the sea-ice extent, as they are directly altered by the overlying atmosphere - a connection that is further explored in Sect. 3.2.

Experiments conducted with a nudged ocean (noGrIS_atm and noGrIS_elev_atm) reveal that the dipole in the temperature difference is caused by the changes in the atmospheric circulation due to the difference in GrIS surface elevation (Fig. 2b & c). Altered GrIS surface properties are negligible in winter for three reasons (Fig. 2d): First, despite the absence of a glacier mask, the presence of a seasonal snow cover during winter limits temperatures to the melting point. Second, the snow cover increases the surface albedo to values similar to those observed in glacier-covered areas and therefore to the albedo in noGrIS_elev, where the glacier mask is retained. Third, the already low daily-mean insolation in Greenland during winter minimizes the significance of the surface-albedo effect. In contrast, the ocean contributes to a cooling, which is largest across the Nordic Seas and associated with the lower GrIS elevation (Fig. 2g). The cooling in the Nordic Seas spreads across the Northern Hemisphere and leads to an increase in sea-ice concentration and thickness (Fig. 2g). As a result, the expanded sea-ice cover and fewer leads in the Northern Hemisphere sea ice reduce the heat loss of the ocean to the atmosphere, thus creating a negative feedback loop on air temperature. The GrIS surface-property effect yields the opposite feedback: Warmer air temperatures, strongest over the Labrador Sea, lead to a lower sea-ice cover in all seasons which allows for a higher heat loss of the ocean towards the atmosphere (positive feedback). Together, both effects lead to an overall negative temperature feedback by the ocean, with the

https://doi.org/10.5194/esd-2024-24
Preprint. Discussion started: 22 August 2024


Earth System Dynamics Discussions
Open Access
EGU

only exception in the Labrador Sea and subpolar gyre (Fig. 2f). Without considering the warming contribution due to the altered surface-properties over Greenland, the region would be colder by up to -2.1 K (noGrIS_elev - noGrIS). As the drivers of the dipole in the 2 m air temperatures can be associated with changes in the atmospheric circulation, they are further investigated in Sect. 3.1.2.

https://doi.org/10.5194/esd-2024-24
Preprint. Discussion started: 22 August 2024

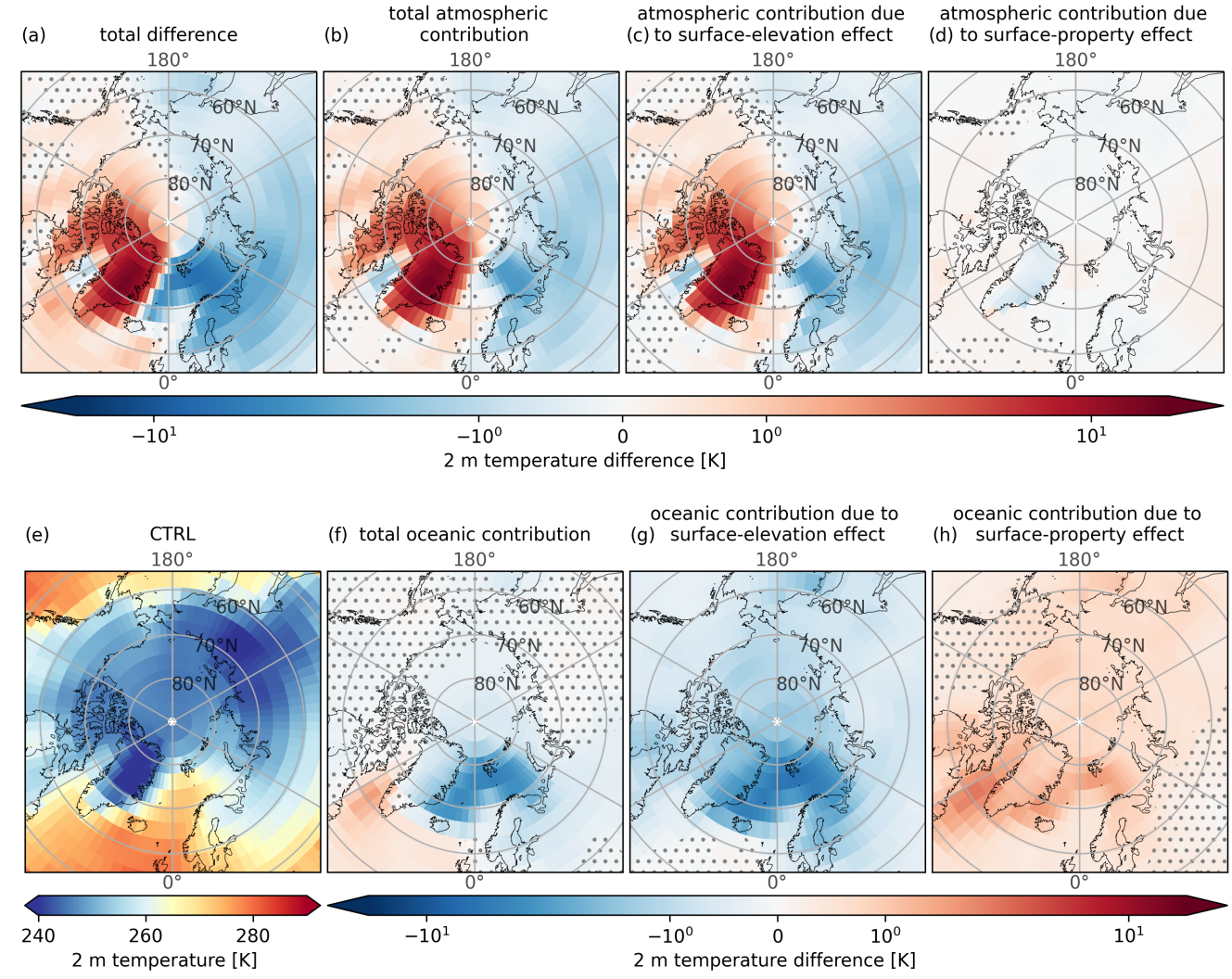

Figure 2. 2 m air-temperature in DJF. (a) shows the total difference (noGrIS - CTRL), (b) the total atmospheric contribution (noGrIS_atm - CTRL_atm), (c) the atmospheric contribution due to the GrIS surface-elevation effect (noGrIS_elev_atm - CTRL_atm), (d) the atmospheric contribution due to the GrIS surface-property effect (noGrIS_atm - noGrIS_elev_atm), (e) CTRL in absolute values, (f) the total oceanic contribution ((noGrIS - CTRL) - (noGrIS_atm - CTRL_atm)), (g) the oceanic contribution due to the GrIS surface-elevation effect ((noGrIS_elev - CTRL) - (noGrIS_elev_atm - CTRL_atm)) and (h) the oceanic contribution due to the GrIS surface-property effect (((noGrIS - CTRL) - (noGrIS_atm - CTRL_atm)) - ((noGrIS_elev - CTRL) - (noGrIS_elev_atm - CTRL_atm)). Stippling indicate regions that are not statistically significant at a significance level (α) greater than 5 %.

Summer

In summer, contributions are comparable, albeit significantly weaker than in winter (Fig. 3). Differences include the absence of a dipole pattern in the atmospheric contribution (Fig. 3b-d) and the emergence of a distinctly positive anomaly over Greenland

https://doi.org/10.5194/esd-2024-24
Preprint. Discussion started: 22 August 2024


Earth System Dynamics Discussions
Open Access
EGU

(Fig. 3a). This anomaly is attributed to the impact of the GrIS surface-property effect on the atmosphere: The removal of the glacier mask and the absence of snow during summer, allow surface temperatures in the simulations without GrIS to exceed the melting point (Fig. 3d). Additionally, they lead to a lower surface albedo, which allows for a higher absorption of solar radiation.

Annual mean

Tallying up the positive and negative anomalies across the Northern Hemisphere, the net difference in the annual 2 meter air temperature between noGrIS and CTRL approaches zero (-0.02 K). Removing the orography of the GrIS leads to a reduced global-mean sea-level pressure and a -0.3 K cooler Northern Hemispheric 2 m air temperature. This is evident from the sensitivity experiment noGrIS_elev, in which only the GrIS elevation effect has been considered. The interplay of altered GrIS surface properties, including surface temperatures rising above the melting point, the growth of vegetation, variations in radiative heating and surface roughness, exerts a counteractive warming effect.

https://doi.org/10.5194/esd-2024-24
Preprint. Discussion started: 22 August 2024

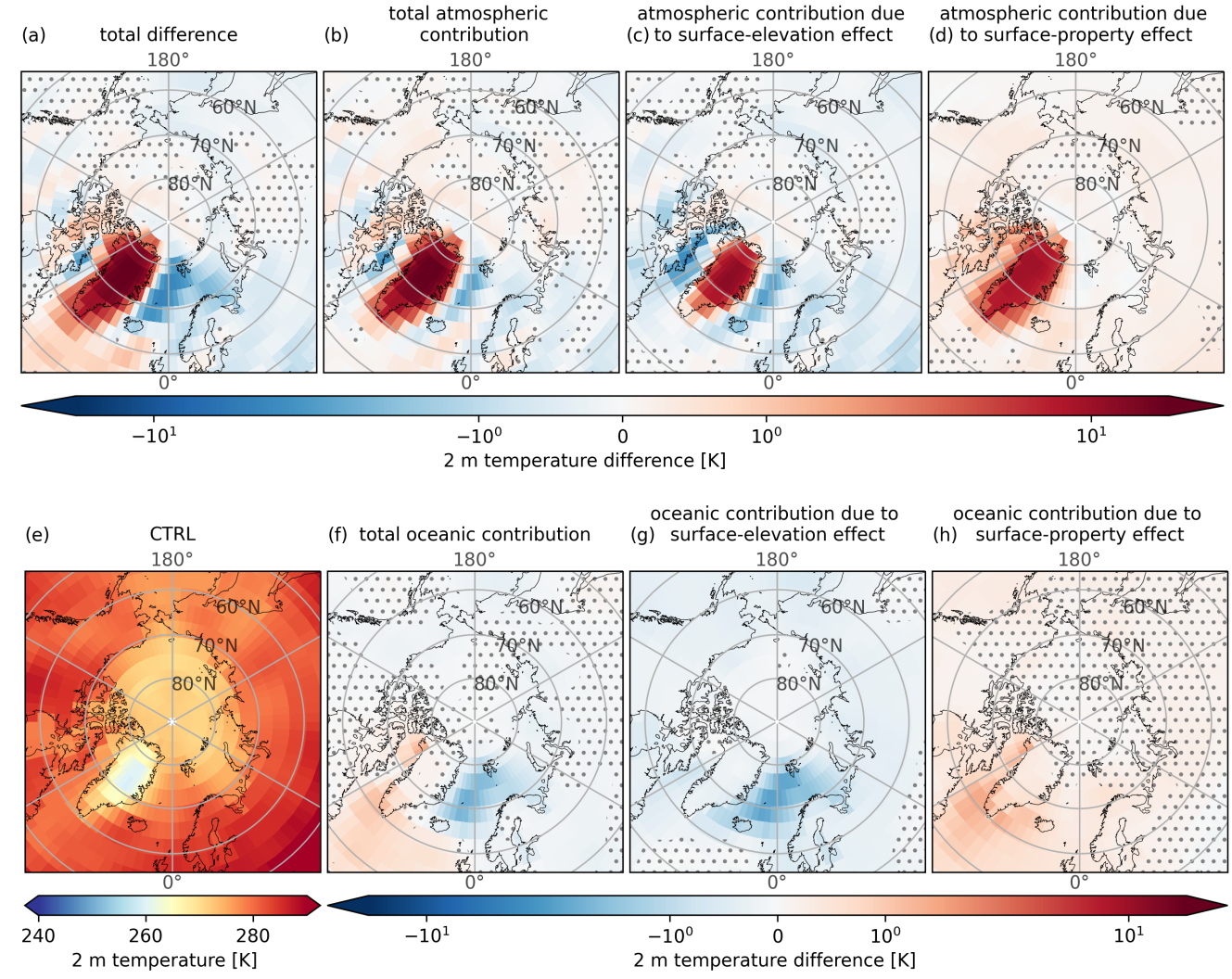

Figure 3. 2 m air-temperature in JJA. For more details on the calculation see Fig. 2. Stippling indicate regions that are not statistically significant at a significance level (α) greater than 5 %.

3.1.2 Dynamic response

Greenland Anticyclone and near-surface winds

In CTRL, the frigid conditions over Greenland create a favorable environment for the formation of a prominent high-pressure system known as the Greenland Anticyclone (Hobbs, 1945) (Fig. 4a). On the other hand, a low-pressure system, referred to as Icelandic Low, resides in the route of dynamic cyclones over the warmer ocean around the tip of Southeast Greenland and Iceland (Serreze et al., 1997). The absent GrIS causes differences in the atmospheric circulation in winter. In noGrIS, the lower orography and removed glacier mask, along with associated 2 m air warming, and the missing mechanical blocking, result in

https://doi.org/10.5194/esd-2024-24
Preprint. Discussion started: 22 August 2024

a weaker Greenland Anticyclone. Concurrently, this reinforces the Icelandic Low (not shown). Due to the weaker Greenland Anticyclone, a notable difference in the strength and direction of annual 10 m winds over Greenland and its vicinity is visible in Figure 4c. In noGrIS, 10 m winds are reversed and take a stronger easterly zonal direction over Greenland as compared to CTRL (Fig. 4b). Originating from a warmer Greenland, when traversing the Baffin Bay towards the Canadian Arctic, they raise 2 m temperatures and contribute to an intensified sea-ice melt in the western Arctic (Sect. 3.2). The pronounced summer warming experienced across Greenland in noGrIs due to the removed glacier mask results in the inflow of significantly warmer winds from Greenland into the Labrador Sea and Baffin Bay, heating the surface ocean and reducing sea-ice cover in summer. This heat absorbed in summer, keeps ocean temperatures warmer throughout the entire year in noGrIS, as compared to the experiment considering only a lower surface elevation (noGrIS_elev). Hence, sea-ice formation is reduced in fall and winter in the Labrador Sea in noGrIS. The resulting lower sea-ice cover allows for even more heat to be stored in the Labrador Sea in summer. In winter, the reduced sea-ice cover decreases the insolation of the ocean, leading to stronger heat loss of the ocean, amplifying the atmospheric warming (Fig. 2h). The warmed Labrador Sea also compensates for some of the cooling effect of the Nordic Seas associated with the lower GrIS surface elevation (Fig. 2g), enhancing the winter warming in Greenland with respect to noGrIS_elev, where the Labrador Sea warming is absent due to the prescribed glaciated surface. The warming effect of altered Greenland surface properties is strongest in the Labrador Sea, yet extends beyond this region, resulting in an overall positive oceanic response (Fig. 2h).

Around Greenland, annual-mean 10 m winds are weaker in the absence of the GrIS (Fig. 4b), decreasing the wind-stress curl on the ocean surface. The strength of the northeast winds over the east coast of Greenland decreases by up to 97 % (-5.7 ms^{-1}) and by up to 80 % over the adjacent East Greenland Current (-4.3 ms^{-1}). Over the Barents Sea and northern Scandinavia, winds are slightly stronger and adopt a more northerly trajectory (Fig. 4c). This facilitates the transport of cold polar air towards lower latitudes. The atmospheric impact becomes evident in the sensitivity experiments with a nudged ocean (noGrIS_atm), revealing a lower winter 2 m air temperature of up to -2.6 K in the Nordic Seas, as shown in Fig. 2b. The stronger and more northerly 10 m winds over the Nordic Seas change the wind stress on the surface and lead to a more southward drift of sea ice, resulting in an expanded sea-ice cover in noGrIS relative to CTRL (further investigated in Sect. 3.2.1). A more southward expansion of the sea-ice cover is also supported by the atmospheric cooling (Fig. 2b). The larger sea-ice extent reduces the heat loss of the ocean and enhances the cooling of the overlying atmosphere. Hence, when accounting for the oceanic feedback, the 2 m winter air temperature experiences a considerable decrease over the Nordic Seas compared to the simulation with a nudged ocean (noGrIS_atm), adding up to a total difference of up to -6.0 K in noGrIS relative to CTRL (Fig. 2a & f). In noGrIS_elev, the temperature difference in the Nordic Seas is even larger (up to -7.5 K in Fig. 2g) as the lower Northern Hemisphere mean temperature favors a stronger sea-ice expansion. Although sea-ice cover expansion, driven by the wind-stress changes induced by the lower GrIS elevation, is most pronounced in the Nordic Seas, it is not limited to that region. This expansion affects also other regions in the Northern Hemisphere, resulting in an overall negative temperature response of the ocean (Fig. 2g). The response of the sea ice is further explored in Sect. 3.2. Being mostly driven by the mere GrIS height reduction, differences in 10 m winds are similar in both, noGrIS and noGrIS_elev (Fig. 4c & d).

https://doi.org/10.5194/esd-2024-24
Preprint. Discussion started: 22 August 2024

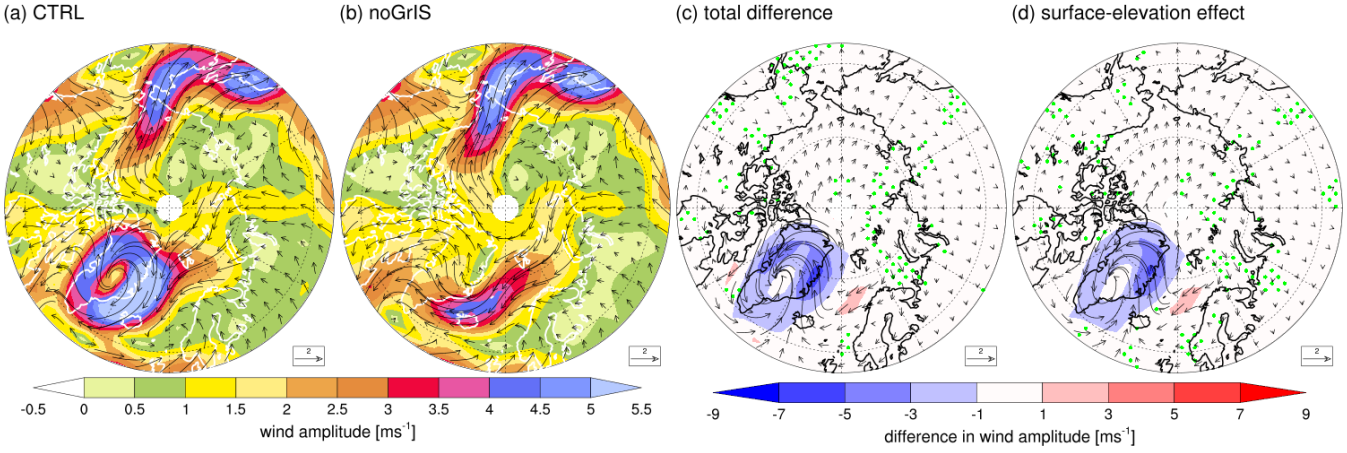

Figure 4. (a-b) Annual 10 m wind amplitude (contours) and direction (vectors, ms^{-1}), (c-d) total difference (noGrIS - CTRL) and surface-elevation effect contribution (noGrIS_elev - CTRL) to the difference in the 10 m wind amplitude. Stippling designates statistically non-significant regions (α>5 %).

Quasi-static wave

In the absence of the blocking GrIS topography, the quasi-static wave at 500 hPa is shifted northeastward over Greenland, while the dominant atmospheric wave number remains unchanged (Fig. 5). This shift results in a stronger meridional flow pattern, characterized by an enhanced southerly wind direction over Greenland and a more northerly wind direction over the Nordic Seas (Fig. 5c). This amplifies the influx of cold polar air towards the Nordic Seas and northern Scandinavia. As air masses are able to penetrate further into the interior of Greenland, they transform the circulation from a "flow around" into a more quasi-geostrophic "flow over" circulation, following Hakuba et al. (2012). The difference in the quasi-static wave is caused by the orographic effect, as suggested by similar patterns in noGrIS and noGrIS_elev (Fig. 5c & d). The GrIS surface-property effect slightly counteracts the normalized geopotential height reduction over Greenland.

https://doi.org/10.5194/esd-2024-24
Preprint. Discussion started: 22 August 2024

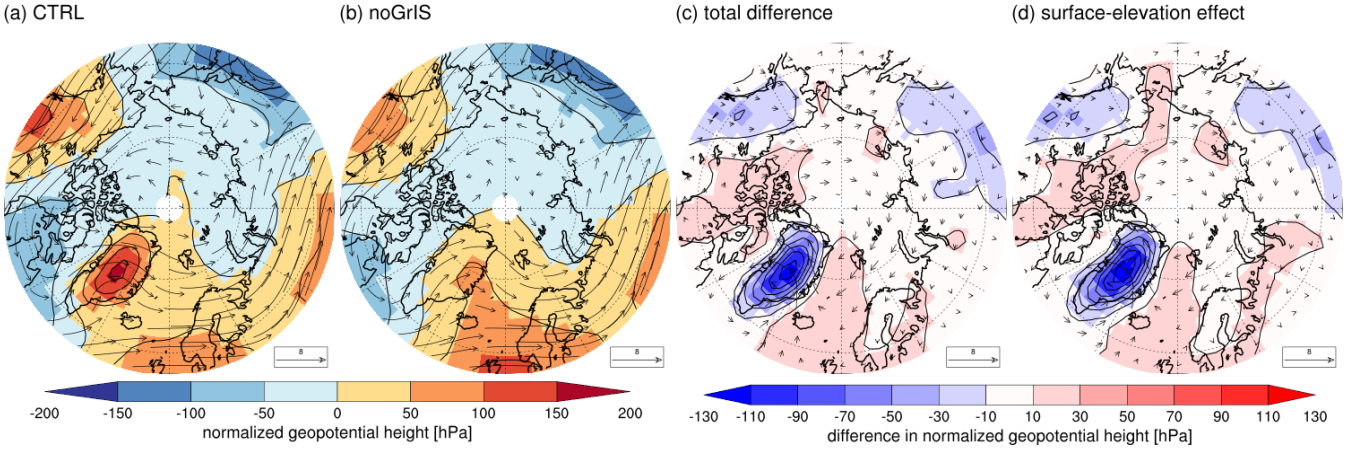

Figure 5. (a-b) DJF normalized geopotential height (contours) and flow direction (vectors, ms^{-1}) at 500 hPa, (g-h) total difference (noGrIS - CTRL) and surface-elevation effect contribution (noGrIS_elev - CTRL) to the difference in the normalized geopotential height and flow direction at 500 hPa. Note that the entire region shown is statistically significant at α=5 %.

Storm tracks and precipitation

Differences in the large-scale circulation patterns also affect the trajectory of winter storm tracks in the Northern Hemisphere. In CTRL, the storms approaching Greenland, as they move from North America to Europe, are diverted south due to the high orography of the GrIS. Hence, storms pass Greenland mainly on its southern edge (Fig. 6a). Additionally, the pressure gradient between the Icelandic Low and the Greenland Anticyclone induces strong easterly onshore winds in Southeast Greenland (Fig. 4a), which are associated with high amounts of precipitation. This is in line with Ohmura and Reeh (1991). Both of these dynamic effects contribute to orographic precipitation in the luv of the mountains and explain the precipitation peak east of Greenland as well as in the southern and southeastern areas of Greenland (Fig. 7a). Characterized by the highest elevation and the coldest air temperatures, the interior of Greenland encounters mostly dry conditions.

In absence of the blocking GrIS, storms penetrate deeper into Central Greenland. This is evident by a higher cyclonic activity over Greenland in noGrIS (Fig. 6b & c). noGrIS reveals a lower frequency of storms over Greenland when compared to noGrIS_elev, implying a contrasting influence of the altered GrIS surface properties on storm tracks. As more storms pass over Greenland in noGrIS, cyclonic activity decreases in the luv of Greenland, specifically over the Canadian Arctic Archipelago, Baffin Bay, parts of Canada. Cyclonic activity increases slightly in the lee of Greenland, specifically over the Nordic Seas and northern Europe. The higher frequency of storms to the southeast of Greenland also explains some of the warmer 2 m air temperatures in this region in noGrIS (Fig. 2b), as storms usually carry not only moist but also warm air masses. In the Nordic Seas, this warming effect is overcompensated by the intensified inflow of cold polar air. Lastly, the stronger storm activity over Greenland contributes to the aforementioned weaker Greenland Anticyclone and the deeper Icelandic Low. As fewer storms reach eastern Siberia, the Siberian High expands (not shown).

https://doi.org/10.5194/esd-2024-24
Preprint. Discussion started: 22 August 2024

Earth System Dynamics
Discussions
Open Access
EGU

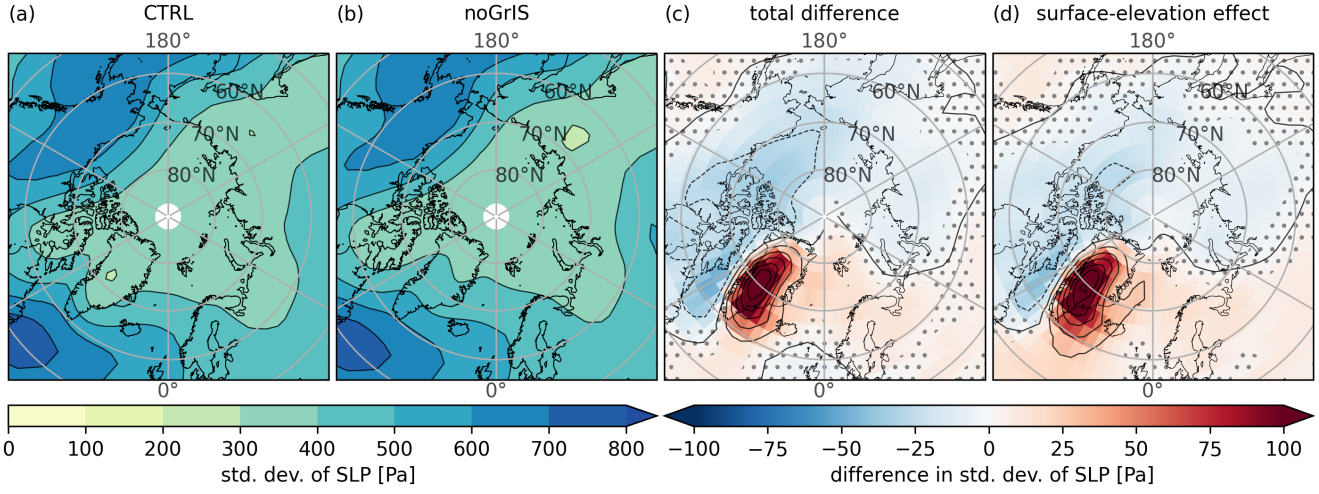

Figure 6. (a-b) Standard deviation of the DJF 2 to 5 days band-pass-filtered sea-level pressure (SLP) as a measure of cyclonic storm activity similar to Dethloff et al. (2004). (c-d) Total difference (noGrIS - CTRL) and surface-elevation effect contribution (noGrIS_elev - CTRL) to the differences in storm activity. Stippling designates statistically non-significant regions (α>10 %).

The shifted quasi-static wave pattern and storm tracks redistribute the annual regional precipitation more homogeneously across Greenland (Fig. 7c & d): Precipitation decreases in the south and southeast of Greenland while increasing in the northeast, where the air masses are forced to lift along the remaining orography. Reduced GrIS blocking also causes an increase in precipitation over the adjacent ocean to the southeast of Greenland. The drier conditions over the northeastern Greenland Sea and western Barents Sea are a consequence of the lower SST, and the stronger northerly flow direction, advecting colder and drier air masses, while reducing the inflow of warm and moist Atlantic air. The situation is reversed for the Labrador Sea, where higher 2 m air temperatures contribute to an increase in evaporation and precipitable water.

The similarity of the patterns over Greenland and east of Greenland in Figures 7c and d suggests that the main contribution stems from the lower GrIS elevation. In the Labrador Sea, altered GrIS surface properties have a compensating effect on storm activity. The same applies to precipitation, where GrIS surface properties dominate only the signal in the Labrador Sea, leading to a wettening due to the stronger summer warming (Fig. 3h & Fig. 7c).

https://doi.org/10.5194/esd-2024-24
Preprint. Discussion started: 22 August 2024

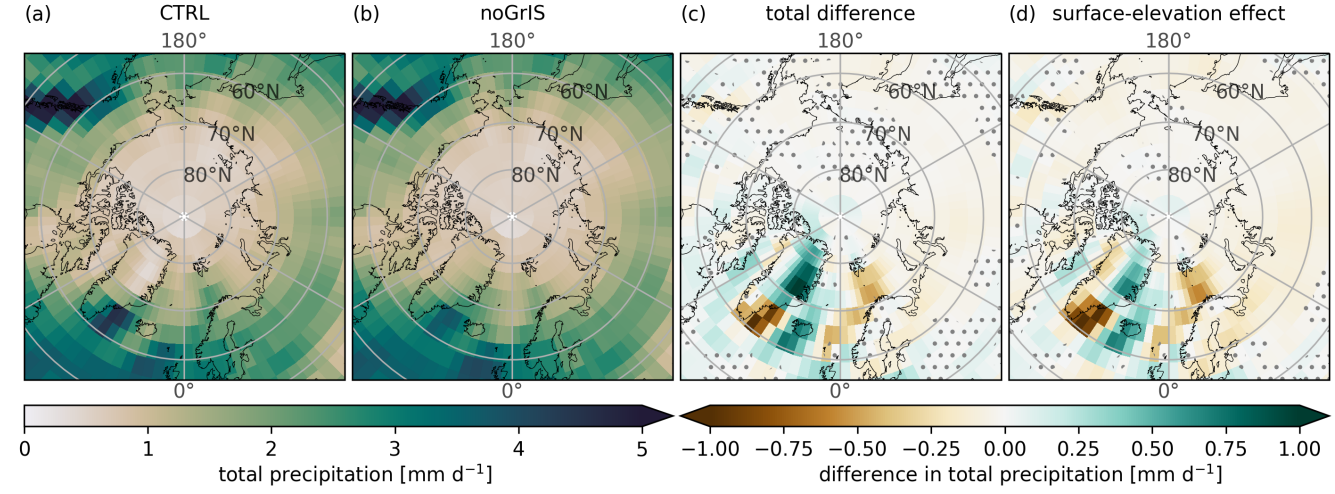

Figure 7. (a-b) Annual-mean total precipitation, (c-d) total difference (noGrIS - CTRL) and surface-elevation effect contribution (noGrIS_elev - CTRL) to the differences in precipitation. Stippling designates statistically non-significant regions (α>5 %).

The redistribution in precipitation also affects river runoff. In noGrIS, less discharge occurs off the south coast of Greenland, whereas an increased discharge occurs off the east coast. The slightly lower precipitation over Eurasia and North America (Fig. 7c) also reduces the runoff of Ob, Yenisey and Lena, and the Mackenzie river. The effects of the changed runoff on the surface ocean are discussed in Sect. 3.2.

3.1.3 Drivers of the Greenland warming

We showed in the previous sections that in absence of the GrIS temperatures over Greenland increase drastically. This warming is not just a direct consequence of the lowered GrIS surface elevation, but atmospheric dynamics and feedbacks from the ocean play a crucial role for the simulated temperature differences between noGrIS and CTRL. Here, we investigate the drivers of the strong warming across Greenland throughout the year. For this, we isolate the atmospheric and oceanic impact by calculating individual contributions from the sensitivity experiments. The results are illustrated in Fig. 8.

Winter

Throughout all seasons, the temperature difference across Greenland is dominated by a positive atmospheric and a weak predominantly negative ocean contribution. In winter, a strong warming relative to CTRL originates from the lower elevation of 1,320 m of the GrIS (+9.6 K), encompassing two distinct effects. The first is the lapse-rate effect, which accounts for the rise in 2 m air temperature due to the lower GrIS surface elevation. The second is an atmospheric circulation effect, such as the prevalence of more southerly high-altitude winds over Greenland and the increase in storm activity (Sect. 3.1.2). Altered GrIS surface properties only have a minor impact on the atmosphere in winter (-0.3 K) as explained in Sect. 3.1.1. The oceanic response to the lower GrIS elevation is negative (-1.8 K), whereas it is positive (1.1 K) in response to the altered GrIS sur-

https://doi.org/10.5194/esd-2024-24
Preprint. Discussion started: 22 August 2024

face properties as consequence of summer conditions (Sect. 3.1.2). Hence, the total winter temperature difference in noGrIS amounts to +8.6 K with the primary influence attributed to the GrIS elevation effect (+7.8 K).

Summer

During summer, large-scale atmospheric variability is low, leading to a lower contribution from elevation-induced atmospheric effects (+5.9 K relative to CTRL) than in winter. A crucial factor during this season is the variable land surface (+7.1 K), which becomes more important due to the exposure of darker surfaces in the absence of a snow cover. The ice-free ground, accompanied by more favorable climatic conditions, promotes the growth of grass and deciduous shrubs, specifically in the northeast of Greenland. This renders Greenland's vegetation similar to that found in the Siberian tundra. The vegetation further lowers the surface albedo in affected regions in Greenland, decreasing the surface albedo by up to -0.6 in noGrIS compared to CTRL. In contrast, CTRL maintains high surface-albedo values and surface temperatures limited to the melting point throughout the summer due to the prescribed ice sheet and its high surface elevation. In noGrIS, surface temperatures above freezing intensify radiative heating and alter the surface-energy budget. Additionally, surface roughness increases in noGrIS; however, a prior study suggests that this has a negligible impact on temperature anomalies compared to the changes in surface albedo (Stone and Lunt, 2013). The cooling effect of the ocean due to the lower GrIS elevation is counteracted by the additional heat stored in the ocean due to the warming of Greenland in response to the surface property changes (Fig. 2h & 3h, Sect. 3.1.2). This is visible in the flipped sign of the oceanic contribution from negative in response to the lower GrIS elevation to positive in response to the altered surface properties over Greenland in Fig. 8. In total, noGrIS summer warming over Greenland amounts to approximately +13.1 K.

Annual mean

In the annual-mean, the 2 m temperature over Greenland warms by +10.7 K. The temperature change is dominated by the atmospheric GrIS elevation effect (+8.3 K), but enhanced by the atmospheric GrIS surface-property effect. The atmospheric warming is counteracted by a slight ocean-induced cooling of -0.3 K.

https://doi.org/10.5194/esd-2024-24
Preprint. Discussion started: 22 August 2024

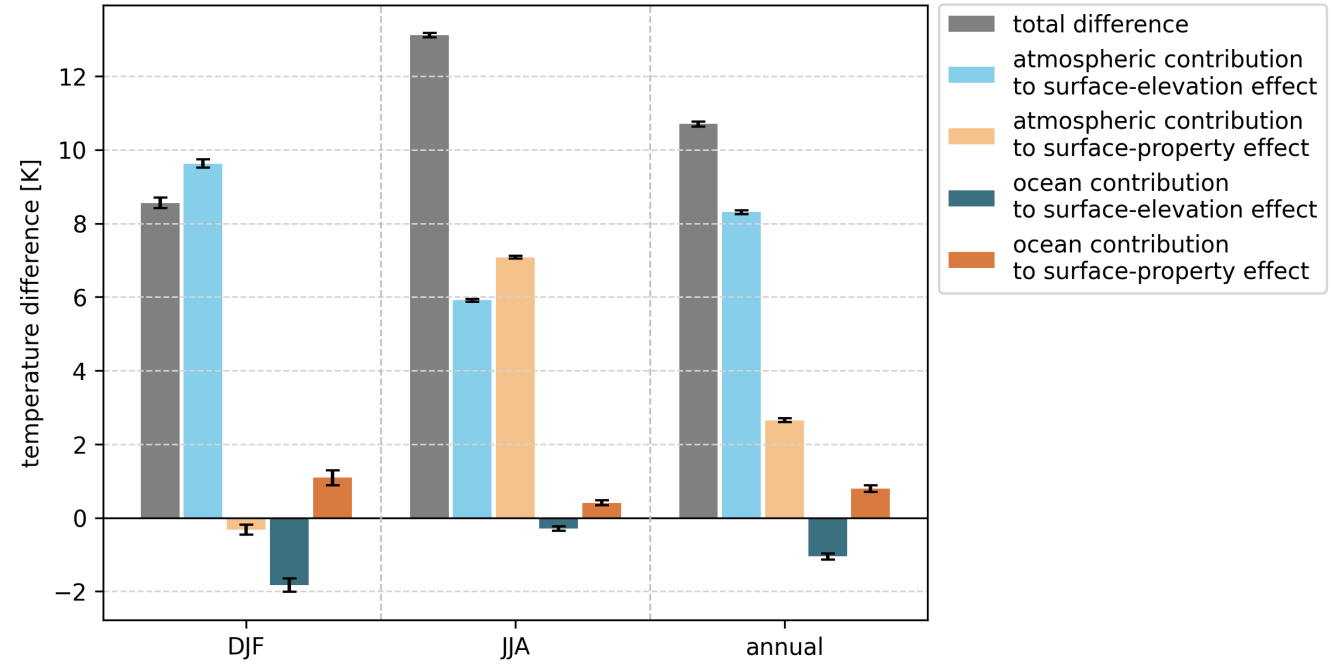

Figure 8. Atmospheric and oceanic contributions to the total 2 m air-temperature difference (grey) averaged over Greenland in DJF, JJA and annually due to the altered GrIS surface elevation (blue) and surface properties (orange). Grey bars illustrate the total difference (noGrIS - CTRL). Light blue bars show the atmospheric contribution due to the lower surface elevation (noGrIS_elev_atm - CTRL_atm). Light orange bars depict additional atmospheric effects arising from the altered GrIS surface-properties (noGrIS_atm - noGrIS_elev_atm). Dark blue bars represent the oceanic contribution due to the lower surface elevation ((noGrIS_elev - CTRL) - (noGrIS_elev_atm - CTRL_atm)). Dark orange bars depict the oceanic contribution due to the altered surface properties ((noGrIS - CTRL) - (noGrIS_atm - CTRL_atm)) - ((noGrIS_elev - CTRL) - (noGrIs_elev_atm - CTRL_atm)). Black whiskers designate the 90 % confidence interval.

3.2 Ocean response and feedback

The preceding analysis indicates that the GrIS significantly impacts the atmosphere through dynamical and thermodynamical processes. This manifests, for instance, in differences in the 2 m air temperature, precipitation and wind stress across the Arctic and sub-Arctic region between CTRL and noGrIS. The air-temperature pattern directly influences the SST pattern, and vice versa. Differences in precipitation and river runoff affect the spatial distribution of freshwater and contribute to buoyancy changes. Density differences and wind stress force the circulation in the Arctic and the exchange of sea-ice and water-mass between the Arctic Ocean and its adjacent oceans. In view of these direct connections, we investigate the impact of a disintegrated GrIS on the ocean in the subsequent sections.

https://doi.org/10.5194/esd-2024-24
Preprint. Discussion started: 22 August 2024


Earth System Dynamics Discussions Open Access EGU

3.2.1 Regional ocean changes

Large oceanic circulation differences between CTRL and noGrIS unfold in the Arctic Ocean, which is geographically isolated from the surrounding oceans by the extensive land masses in the Northern Hemisphere. This isolation, coupled with the relatively high input of freshwater from precipitation and runoff, creates a distinct salinity gradient between the Arctic Ocean and its neighboring oceans. Exchange of freshwater from the Arctic Ocean with high-salinity water form subpolar oceans and export of sea ice from the Arctic Ocean occurs through five straits. The Fram Strait is the major pathway for fresh polar water and sea ice out of the Arctic, making this strait a significant freshwater sink for the Arctic Ocean in CTRL. Outflow is transported south by the East Greenland Current and exported through the Denmark Strait. Additionally, outflow from the Arctic Ocean takes place via the Nares Strait as well as through the Canadian Arctic Archipelago (hereafter referred to as Canadian Archipelago). The outflow is balanced by the inflow of North Atlantic waters by the Norwegian Atlantic Current through the Barents Sea Section (between Svalbard and Novaya Zemlya) and west of Svalbard as well as by the inflow of Pacific waters through the Bering Strait. The rates at which these exchanges occur influence the characteristics of the Arctic Ocean and adjacent seas. Therefore, we analyze the differences in these rates between CTRL and the experiments with a disintegrated GrIS, summarized in Table 2, for each individual ocean basin in the following.

Arctic Ocean

In noGrIS, the anticyclonic Beaufort Gyre is stronger and more extensive than in CTRL (Fig. 9). Further, its core is slightly shifted towards the southeast (Fig. 10b & f). In the eastern Arctic, this change leads to an intensified flow of water from the Chukchi Sea along the coastline of Siberia towards the Laptev Sea. This circulation pattern favors the advection of fresh water towards the Laptev Sea, while reducing the influx of saline North Atlantic Ocean water into the Laptev Sea. The stronger Beaufort Gyre also transports fresh river runoff from the Eurasian rivers more effectively away from their deltas into the Arctic Ocean, as visible by the changed vectors of flow direction and the freshening north of Eurasia in Fig. 10e-g. As a consequence, eastern Arctic waters are fresher throughout the whole water column in noGrIS than in CTRL (shown for the upper 100 m in Fig. 10g).

In the western Arctic Ocean, the cyclonic coastal current, which originates from the Bering Strait and flows along the Canadian Archipelago towards Lincoln Sea, is weaker in noGrIS (Fig. 9). Therefore, less freshwater is advected towards Ellesmere Island in noGrIS, visible in the positive salinity anomaly close to the northeastern Canadian Archipelago and off the northern coast of Greenland in Fig. 10e-g.

https://doi.org/10.5194/esd-2024-24
Preprint. Discussion started: 22 August 2024

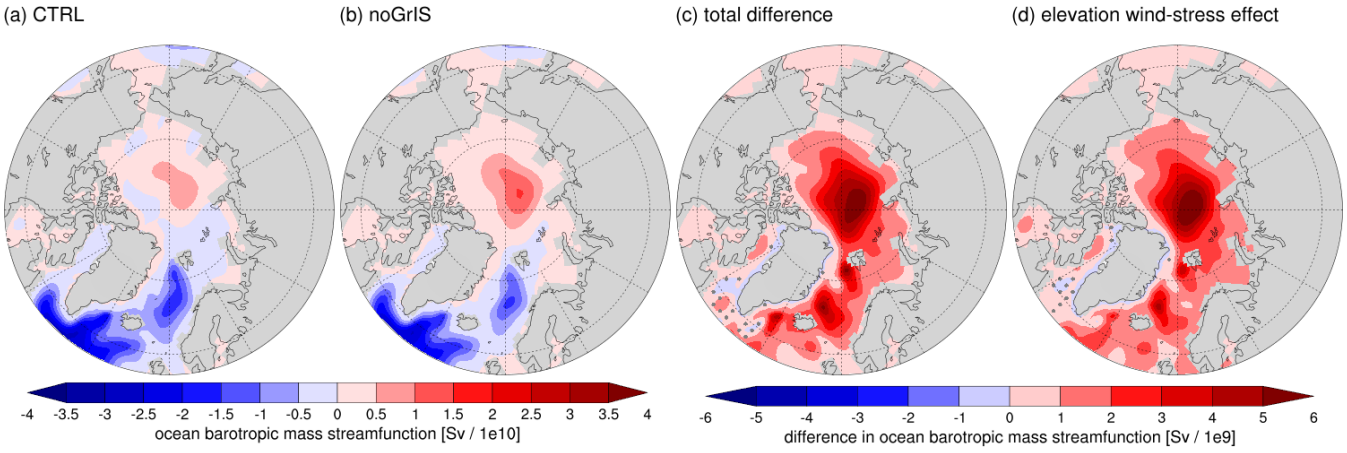

Figure 9. Annual-mean ocean barotropic mass streamfunction. The two left columns show CTRL and noGrIS, the two right columns show the total difference (noGrIS - CTRL) and the wind-stress effect due to the lower GrIS surface elevation (CTRL_wind - CTRL). Stippling designates statistically non-significant regions (α>5 %).

The eastward shift and southward expansion of the southern part of the Beaufort Gyre leads to a twofold export of sea ice through the Barents Sea Section in noGrIS compared to CTRL. Additionally, due to the changed dynamics of the Beaufort Gyre, more sea ice and surface water from the eastern Arctic flow through the Transpolar Drift Stream towards Ellesmere Island and remain in the Arctic Ocean instead of being exported via Fram Strait (Fig. 10b & f). This advects the negative salinity anomaly from the east into the western Arctic Ocean (Fig. 10e-g). In noGrIS, more ocean mass is exported via western Arctic Straits, following the differences in the circulation and a stronger sea-level gradient from the southeastern Arctic Ocean to the northern Baffin Bay (not shown). In contrast to the Barents Sea Section, export of sea ice and water mass through Fram Strait is reduced by 50 %. This reduction is balanced by a concurrent decrease (-33 %) in import of water mass into the Arctic Ocean through the Barents Sea Section, further amplifying the freshening of the Arctic Ocean. Driven by the freshening and warming at levels below 300 m, the density decreases throughout the entire vertical column of the Arctic Ocean (not shown).

The changes in the circulation patterns and the exchange rates between the Arctic and the neighbouring oceans are mostly a consequence of the altered wind stress in response to the lower GrIS elevation. The modified GrIS surface properties only exert an amplifying influence, for example on the strengthening of the Beaufort Gyre (Fig. 10). Differences between the wind-stress sensitivity experiment (CTRL_wind) and the full elevation experiment (noGrIS_elev) indicate that atmospheric circulation changes in response to the lower GrIS elevation compensate for some of the wind-stress-induced changes. Although both, the GrIS surface-elevation and property effect, contribute to the density change, the impact of the surface properties is more pronounced and extensive, particularly below 1,500 m.

Nordic Seas

In the Nordic Seas, the southward expansion of sea ice associated with the wind-stress changes in response to the GrIS elevation reduction leads to a cooling of the upper ocean until around 150 m (Fig. 11). This southward expansion is amplified by the aforementioned higher export of sea ice through the Barents Sea Section and the atmospheric cooling associated with the

https://doi.org/10.5194/esd-2024-24
Preprint. Discussion started: 22 August 2024

stronger northerly wind direction over the Barents Sea (Sect. 3.1.2 & Fig. 2b). The expanded sea-ice cover not only negatively feeds back onto the 2 m air temperature (Fig. 2), it also increases ice melting, and thereby, the freshwater input in the more southerly regions of the Nordic Seas.

The primary driver of the freshening in the Nordic Seas (Fig. 10e-g), however, is the altered ocean currents propelled by the changed wind stress, particularly evident in the weaker wind stress along Greenland's east coast in noGrIS (Sect. 3.1.2). Further, the wind-stress curl on the upper Greenland and Norwegian Sea changes, attenuating the local wind-driven ocean circulation, as evident by a weaker Greenland Sea Gyre (Fig. 9). As a consequence, the influx of North Atlantic waters into the Nordic Seas via the Iceland-Scotland Section is decreased, thereby reducing the salt content of the Nordic Seas. The reduced northward transport of water by the Norwegian Atlantic Current also contributes to the freshening of the Arctic Ocean in noGrIS relative to CTRL. As a consequence, water exported through the eastern Fram Strait is fresher, amplifying the freshening of the Nordic Seas. The freshening is further intensified by enhanced runoff from Northeast Greenland, caused by the precipitation changes (Sect. 3.1.2).

Another contribution to the freshening and cooling in noGrIS stems from an expansion of the East Greenland Current eastward into the Nordic Seas, progressively mixing fresh and cold polar waters with North Atlantic water (Fig. 10e & f). The East Greenland Current is also shallower in noGrIS compared to CTRL, leading to a positive temperature and salinity anomaly close to the shelf region at around 150 m. Both, the widening and the shallowing are dominated by the wind-stress effect.

The freshening, which is strongest at the surface (up to -1.4 psu) and propagates into intermediate and deep layers (>100 m) , enhances the stratification in the Nordic Seas in noGrIS (Fig. 11). As a consequence, heat loss towards the atmosphere is reduced, warming the intermediate and deep ocean (>150 m). The resulting warming at deeper layers is particularly pronounced when also altering GrIS surface properties, as their warming effect on the Northern Hemisphere ocean strengthens the stratification.

Water in the Nordic Seas is lighter in the absence of the GrIS. The density decrease due to the freshening at the surface is larger than the density decrease due to the warming at intermediate and deep layers in noGrIS (Fig. 11). As a consequence, the pycnocline between the surface and intermediate ocean is stronger in noGrIS than in CTRL. This manifests in less deep-water formation within the Nordic Seas in noGrIS. Less upwelling of salty and warm intermediate water intensifies the surface freshening and cooling caused by the altered ocean and atmospheric circulation in noGrIS. This amplifies the buoyancy in the upper ocean. Equally, reduced downwelling of cold surface waters contributes to the warming of the deeper water layers. The reduction in deep-water formation further contributes to the weakening of the Greenland Sea Gyre. The sensitivity experiments indicate that the convection changes in the Nordic Seas are a consequence of the combination of changed transport rates through the Arctic Gateways in response to the altered wind stress (CTRL_wind) and the upper-ocean density changes driven by temperature effects due to the lower GrIS surface elevation (noGrIS_elev, Fig. 12). The GrIS surface-property effect is more important for density changes at intermediate and deep layers through its impact on temperature.

In response to the reduced deep-water formation in the Nordic Seas, the amount and density of overflow into the Denmark Strait decreases. Nearly half of the reduction in the amount is attributed to wind-stress changes caused by the lower GrIS surface

https://doi.org/10.5194/esd-2024-24
Preprint. Discussion started: 22 August 2024

Earth System Dynamics
Discussions
Open Access
EGU

elevation. The altered GrIS surface properties amplify this effect by increasing temperatures and decreasing the density. This results in a total reduction in the amount of dense overflow of -1.3 Sv (-40 %).

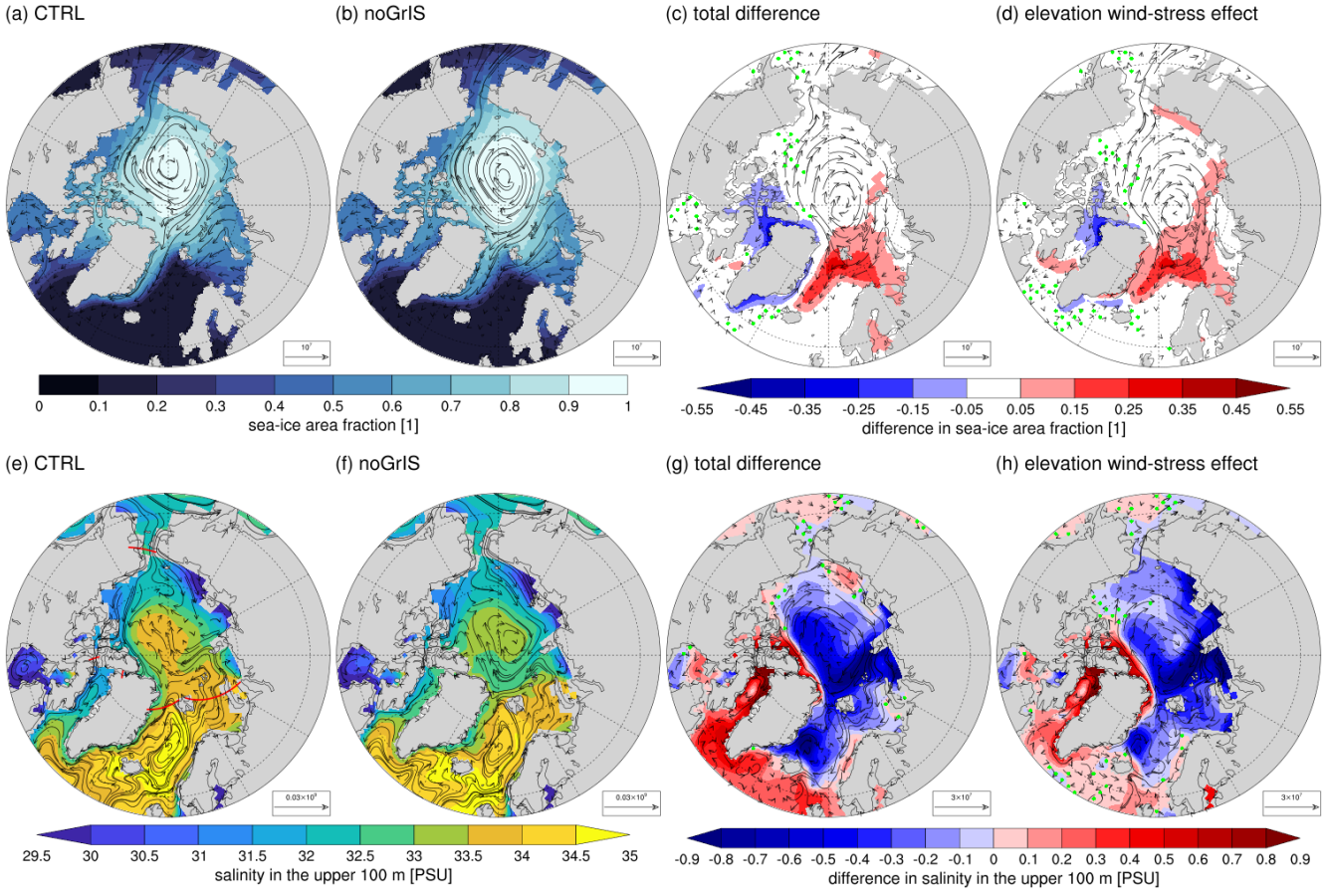

Figure 10. (a-d) Annual-mean sea-ice fraction (contours) overlayed with sea-ice transports (vectors, kg s^{-1}) and (e-h) annual-mean salinity averaged over the upper 100 m (contours) overlayed with water-mass transports (vectors, kg s^{-1}). The two left columns show CTRL and noGrIS, the two right columns show the total difference (noGrIS - CTRL) and the wind-stress effect due to the lower GrIS surface elevation (CTRL_wind - CTRL). Stippling designates statistically non-significant regions (α>5 %). The red lines in e) depict the locations of the transects used for the transport rates in Table 2.

Baffin Bay

Following the change in wind stress due to the lower GrIS elevation, the Arctic water-mass export through Nares Strait doubles, while surpassing the CTRL flow through the Canadian Archipelago by 70 %. As the cyclonic rim current north of the Canadian Archipelago weakens, the exported water increasingly comprises saline water from off the northwest coast of Greenland and off the Canadian Archipelago, rather than fresher Beaufort Sea water as in CTRL. The higher rate of sea-ice formation along the eastern edge of the Canadian Archipelago and the northern Baffin Bay in noGrIS_elev further adds to the higher salinity through

https://doi.org/10.5194/esd-2024-24
Preprint. Discussion started: 22 August 2024

brine rejection as the sea ice is transported southward directly after its formation (Fig. 10b). Additionally, less fresh water is imported into the Baffin Bay by the West Greenland Current, nourished by fresh and cold water from the East Greenland Current. Another contribution to the salinity increase in the Baffin Bay in noGrIS is the slightly lower runoff into Baffin Bay due to higher evaporation over western Greenland (not shown). The resulting positive salinity anomaly extends to a depth of approximately 200 m as the strait in the Canadian Archipelago and Nares Strait both have depths of less than 200 m. The enhanced salinity drives an increase in the production of dense surface water, however, with little effect on deeper ocean layers (>500 m) in the Baffin Bay.

Labrador Sea, Irminger Sea & subpolar gyre

In the Labrador Sea, salinity and temperature are higher throughout the entire vertical column in absence of the GrIS (Fig. 11). The major driver of this change is the stronger advection of saline and warm water from the North Atlantic towards the Labrador Sea: In response to the changed wind stress associated with the lower GrIS elevation, the eastern subpolar gyre circulation is weaker (Fig. 9h), reducing the northward transport of saline and warm water through the Iceland-Scotland Section. A greater portion of the saline North Atlantic water remains within the subpolar gyre, where it moves westward towards the Labrador Sea. Another driver of the increase in temperature and salinity in the Labrador Sea is the reduced export of fresh and cold polar water from the Arctic by the East Greenland Current through the Denmark Strait. This water initially flows into the Irminger Sea before progressing further as West Greenland Current into the Labrador Sea. The reduction is primarily influenced by the changes in wind stress (CTRL_wind, Fig. 10g & h). Furthermore, the exported water through Denmark Strait is warmer and more saline (<150 m) due to the aforementioned changes in the Nordic Seas and the East Greenland Current in the absence of the GrIS. Additionally, the water export from the Baffin Bay through Davis Strait into the Labrador Sea is less fresh in the subsurface 300 m, attributed to the higher salinity in the Baffin Bay as depicted in the previous subsection.

In the subsurface 300 m in the Labrador Sea, density rises strongly together with salinity, caused by the GrIS elevation effect and amplified strongly by the GrIS surface-property effect (Fig. 11). Only in the eastern subpolar gyre, altered GrIS surface properties have a counteractive impact as here their induced warming is stronger than their induced increase in salinity (not shown). At around 300 m depth, density in noGrIS remains nearly unchanged, whereby the influence of the higher temperature (wind-stress changes due to lower GrIS surface elevation and GrIS surface properties) cancels out the density changes due to higher salinity (wind-stress changes due to lower GrIS surface elevation). Persistent warming below 400 m, due to a combination of wind-stress changes and altered GrIS surface properties, causes the density to be lower within the core of the North Atlantic Deep Water (NADW) between 400 and 2,500 m.

In CTRL, a strong pycnocline in the Labrador Sea separates the fresh and cold surface layers from the underlying more saline and warmer layers (Fig. 11). In noGrIS, the pycnocline is weaker due to the higher upper-ocean salinity, increasing the density within the top 300 m. Decreased vertical stability intensifies intermediate and deep convection, which increases the average annual maximum regional mixed-layer depth to 2,500 m in noGrIS compared to 1,600 m in CTRL (Fig. 12). However, convection in the Labrador Sea is subject to strong multi-decadal variability, reaching up to 3,300 m in individual years in noGrIS. Stronger mixing with the underlying more saline and warmer layers amplifies the positive anomaly in upper-ocean salinity and temperature and thereby the buoyancy loss. While convection is also intensified and the local mixed-layer depth

https://doi.org/10.5194/esd-2024-24
Preprint. Discussion started: 22 August 2024

Earth System Dynamics Discussions
Open Access
EGU

increases in the Irminger Sea in noGrIS, this increase is still insufficient to result in deep-water formation. Intensified convection in the Labrador Sea is not only driven by the elevation effect of the GrIS but also considerably by its surface-property effect as it further increases surface salinity.

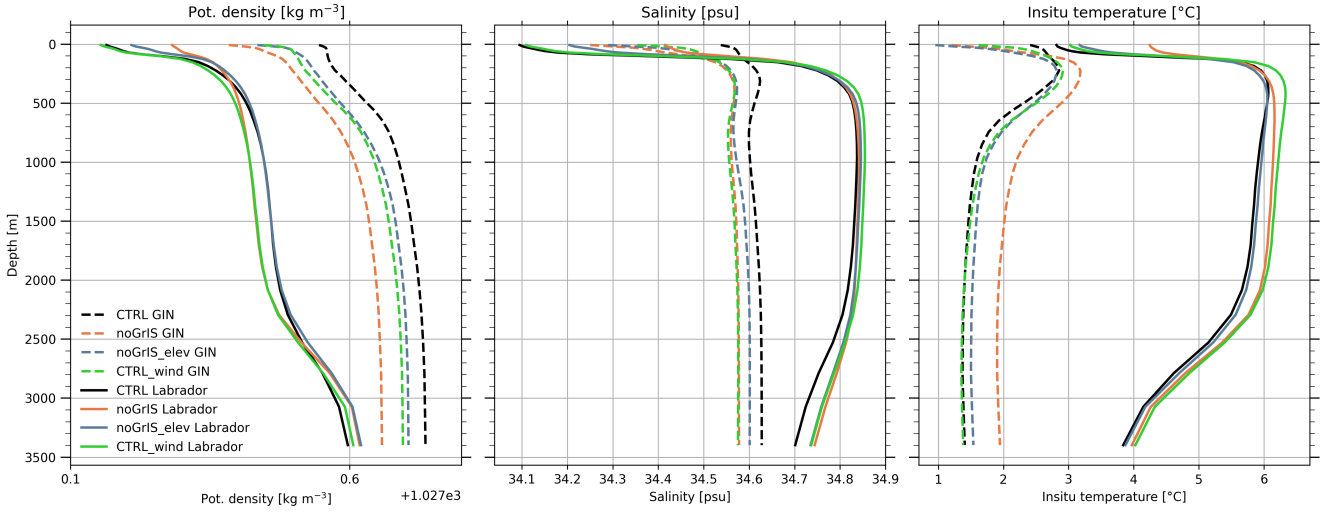

Figure 11. Sea-water potential density in noGrIS (orange), noGrIS_elev (blue) and CTRL_wind (green) compared to CTRL (black) spatially averaged in the region of highest convection in the Nordic Seas (hatched line) and the Labrador Sea (solid line) in March. The regions used to calculate the vertical means are defined in the appendix A1.

Given the reduced deep-water formation within the Nordic Seas and the reduced water-mass export through Denmark Strait, the density of overflow in the Denmark Strait is lower and its amount is decreased by more than half (-1.3 Sv) in noGrIS relative to CTRL. This is partly driven by the lower GrIS elevation but dominated by the impact of altered GrIS surface properties. The decrease in overflow supplied from the Nordic Seas should elevate the likelihood of deep convection and deep-water formation in the Labrador Sea, which is the second key region for deep-water formation in the Northern Hemisphere in our model. Nevertheless, the dense water formed in the Labrador Sea does not fully compensate for the reduced overflow, visible in a decrease in NADW density below 500 m in the Labrador Sea (Fig. 11). At levels below 2,500 m, an upward shift occurs in the transition between NADW and Antarctic Bottom Water (AABW). This shift is tied to the reduced density of NADW in the Labrador Sea, consequently allowing AABW to expand upwards.

But how can the alteration of GrIS surface properties cause a warming at intermediate and deep layers? As mentioned before, one of the main drivers is the change in the ocean circulation in response to the wind-stress changes in absence of the high orography, which is amplified by the GrIS surface-property effect. Another driver is the reduced deep-water formation in the North Atlantic Ocean that reduces the downward transport of cold, dense water. The reduction is partly caused by the lower GrIS elevation, but amplified by the GrIS surface-property effect, due to its contribution to a stronger stratification in the Nordic Seas with less overflow into the Labrador Sea. Furthermore, the upper Labrador Sea is warmer in response to the storage of

https://doi.org/10.5194/esd-2024-24
Preprint. Discussion started: 22 August 2024

Earth System Dynamics Discussions
Open Access
EGU

additional heat from Greenland when removing the glacier mask, causing downward transported water to be comparatively less cold than in CTRL.

3.2.2 GrIS impact on the AMOC

As shown in the previous section, differences in the water-mass properties between noGrIS and CTRL have a significant impact on the deep-water formation in the North Atlantic. This in turn can have substantial consequences for the AMOC strength and thereby the Atlantic heat transport between lower and higher latitudes (Jackson et al., 2015; Liu et al., 2024). We propose that the reduced deep-water formation in the Nordic Seas in noGrIS, leading to a density decrease in NADW, is responsible for local AMOC changes. In the Labrador Sea and the subpolar gyre, the water being formed at the surface lacks sufficient density to sink into the depths. Hence, it cannot compensate for the reduced density at depth that results from a reduced overflow from the Denmark Strait. These changes result in a shift of the lower boundary of the AMOC to shallower depths and prevent the AMOC from extending as far north into the Nordic Seas as in CTRL, while the maximum AMOC strength and depth in the subtropics remain almost unchanged. The shallowing of the AMOC cell is strongest between 40 and 60° N, peaking at approximately -230 m at around 58° N. Both, the GrIS surface-elevation and property effect drive the AMOC cell shallowing and retreat, though the surface-elevation effect dominates the changes. The shallowing is also reflected in the increase of AABW below the subpolar gyre. Similar to the maximum strength of the AMOC, the Atlantic heat transport between 20 and 50° N changes only marginally (<2 %).

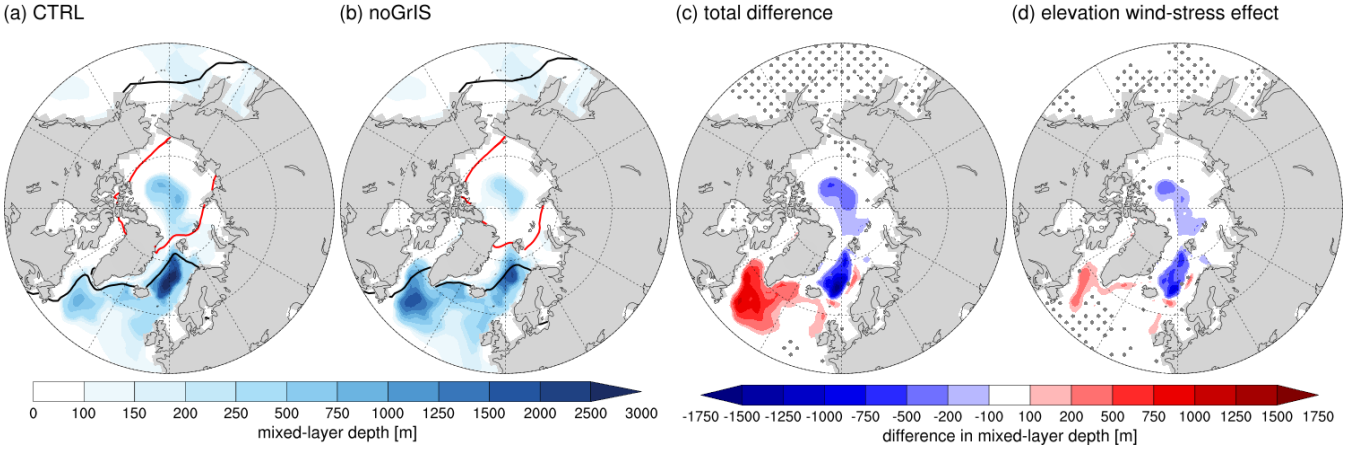

Figure 12. Mixed-layer depth in the North Atlantic. The two left columns show CTRL and noGrIS, the two right columns show the total difference (noGrIS - CTRL) and the wind-stress effect due to the lower GrIS surface elevation (CTRL_wind - CTRL). For each grid cell the annual maximum value is shown. Stippling designates statistically non-significant regions (α>5 %). The red outline shows the minimum sea-ice extent in September and the black line the maximum extent in March. The regions chosen for the computation of the mixed-layer depth are shown in Appendix A1.

https://doi.org/10.5194/esd-2024-24
Preprint. Discussion started: 22 August 2024


Earth System Dynamics Discussions Open Access EGU

3.3 Remote changes

Climatic differences in response to the absence of the GrIS are not limited to the Northern Hemisphere (sub-)polar regions. On a larger scale, the 2 m air temperature dipole pattern in the Northern Hemisphere (Sect. 3.1.1) in response to the atmospheric circulation changes due to the reduced barrier effect of Greenland extends southward, causing cooling over Europe as well (Fig. 13). The cooling is strongest over Scandinavia, but it extends to parts of Central Europe, reaching on average -1.18° C (noGrIS-CTRL). Further, the difference in the atmospheric circulation causes a slight decrease in the storm activity over France, Northwestern Germany and the United Kingdom (not shown).

In the subtropics, weaker zonal winds at around 40° N, in response to the reduced GrIS surface elevation and amplified by the altered GrIS surface properties, slightly shift the North Atlantic subtropical gyre southward (Fig. 13). The displacement leads to an increase in the presence of subpolar water at lower latitudes, reflected in a negative salinity and temperature anomaly in the northern part of the subtropical gyre (not shown). Being slightly more dependent on temperature, the density increases in response to the cooling and the sea level falls (not shown). Due to a contraction, the lower boundary of the North Atlantic subtropical gyre is shallower.

3.4 Disentangling the impact GrIS elevation and surface-property effect

The results presented in this paper show that a disintegration of the GrIS would have substantial implications for atmospheric and oceanic dynamics. Through our set of sensitivity experiments, we elucidate the distinct contributions of various factors involved in the complex interplay among the GrIS, atmosphere and the ocean, as illustrated by the schematic in Fig. 13.

CTRL and noGrIS differ in their Greenland surface elevation (Δ1,320 m on average) and surface properties (i.e., removed glacier mask). The associated thermodynamic and dynamic changes are dominated by the orographic effect. Annual 2 m air temperature significantly increases (+10.7 K) over Greenland in noGrIS, which can to about 68 % be attributed to the GrIS elevation effect. The remaining 32 % of the warming are explained by the modification of GrIS surface properties. Of this effect, half is ascribed to the lower surface albedo, while the other half is linked to the removal of the glacier mask, allowing surface temperatures to surpass the melting point. Note however, that in the case of the annual 2 m air temperature over Greenland, ocean feedbacks slightly counteract the overall warming, as discussed in Section 3.1.3. A lower GrIS elevation also reduces the mechanical blocking with significant implications for the atmospheric circulation: 84 % of the weakening of the Greenland Anticyclone are due to the GrIS elevation effect, lowering the amplitude and altering the direction of Arctic 10 m winds. The lower elevation contributes to 82 % of the weaker 10 m winds east of Greenland, while altered GrIS surface properties explain the remaining 18 %. Weaker blocking further leads to a northeast shift of the 500 hPa quasi-static wave, intensifying southerly wind flow over Greenland and northerly flow over the Nordic Seas. While the shift in the 500 hPa quasi-static wave is caused entirely by the elevation effect, it is noteworthy that the surface properties have an opposing effect on this wave shift. The changes in the quasi-static wave favor the Arctic SST and 2 m air-temperature dipole, explaining the cooling over Central and Northern Europe. Lastly, the reduction of the orographic barrier enables cyclones to penetrate farther into Greenland, redistributing precipitation.

https://doi.org/10.5194/esd-2024-24
Preprint. Discussion started: 22 August 2024

Changes in the wind stress, due to the lower GrIS elevation, cause a stronger and eastward-shifted Arctic Ocean gyre and a weaker wind-driven ocean circulation in the Nordic Seas. This enhances sea-ice export through the Barents Sea Section, the Nares Strait and the Canadian Archipelago, while reducing the export through Fram Strait (Fig. 13). Additionally, water exchange between the Arctic Ocean and its neighboring oceans decreases east of Greenland and increases west of Greenland. As the GrIS surface-property effect amplifies the wind-stress disparities, it also intensifies most of the differences in the oceanic transport. Notably, the GrIS elevation effect accounts for the majority of the reduction in the export via Fram Strait, 94 % of the water-mass and 75 % of the sea-ice transport differences between noGrIS and CTRL. The contribution of the GrIS elevation effect accounts for 77 % of the higher water-mass and 89 % of the higher sea-ice export via Nares Strait. In the Canadian Archipelago 80 % of the higher water-mass and but only 48 % of the higher sea-ice export are caused by the GrIS elevation effect. Here, the GrIS surface-property effect more strongly amplifies the transport differences. An exception is the exchange via the Barents Sea Section and Bering Strait, where changed GrIS surface properties have a counteractive effect on the water-mass import and the sea-ice export. While being minor for the sea-ice transport and water transport changes through the Barents Sea Section, the GrIS surface-property effect dominates the changes in water import through Bering Strait and overcompensate for the contradicting GrIS surface-elevation effect.

The alterations in ocean-mass transports, driven by changes in the wind stress, are the primary cause of the changes in ocean properties at Northern Hemisphere's convection sites. Thereby they considerably impact density variations that are crucial for convective processes. In the Nordic Seas, the lower GrIS elevation is the main contributor to the fresher surface layers in noGrIS, comprising 75 %. Its impact on density decreases with depth, accounting for on average 44 % of the density decrease in the surface layers and 37 % in the deeper layers. Instead, the GrIS surface-property effect dominates the warming and density decrease at deeper layers. It even overcompensates the GrIS surface-elevation-induced cooling and leads to a total warming at intermediate and deep layers. Similarly, the lower GrIS elevation is the sole reason for the shallowing of the mixed-layer depth, with around 42 % of the shallowing attributed to the altered wind stress. As the density decrease at deeper layers is predominantly driven by GrIS surface-property-induced warming, also the reduction in the amount and density of overflow from the Denmark Strait is strongly tied to the GrIS surface-property effect, accounting for 54 % of the reduced amount. In the upper Labrador Sea, altered GrIS elevation has an important impact on the salinity and density increase, contributing 46 % and 60 %, respectively. In contrast, GrIS surface properties crucially determine the warming (77 %) at deeper layers and thereby even overcompensate for the density-increasing effect of the higher salinity in noGrIS_elev. The deepening of the mixed-layer depth in the Labrador Sea is primarily driven by the lower surface elevation, which accounts for more than two-thirds of the effect (79 %), while the altered surface properties contribute to a lesser extent, making up 21 % of the influence. The lower GrIS elevation dominates the shallowing of the lower boundary of the AMOC between 40 and 60° N by 60 %, although variability between years leads to a relatively high uncertainty of 15 %. A comparison of the here analyzed 1,000 year period with the two preceding thousand-year intervals (5,000-5,999 and 6,000-6,999) for the respective experiments indicates that the contributions to the shallower AMOC cell are not entirely robust (not shown).

https://doi.org/10.5194/esd-2024-24
Preprint. Discussion started: 22 August 2024

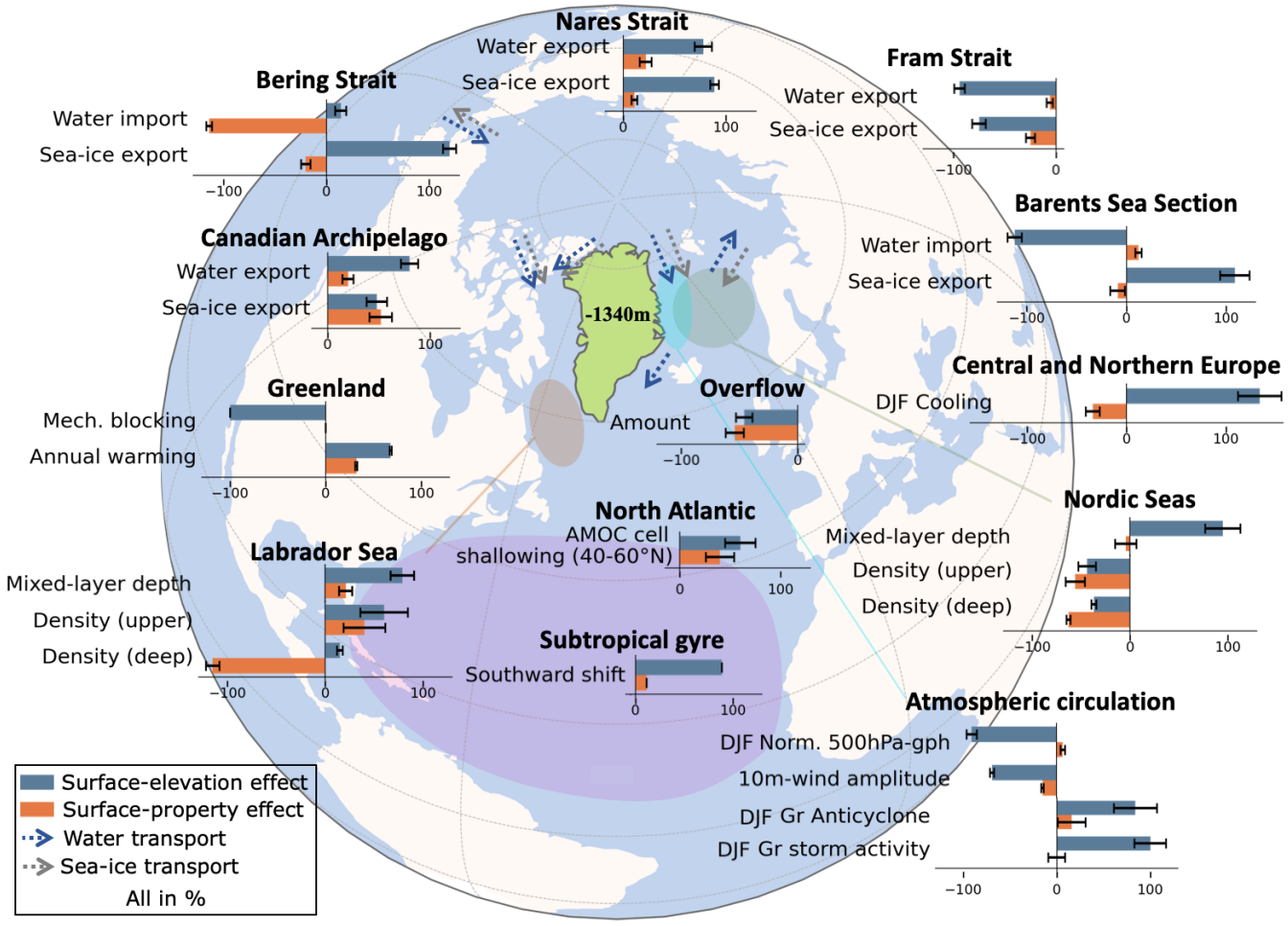

Figure 13. Contribution of the GrIS surface-elevation (blue) and the GrIS surface-property effect (orange) to the simulated climate changes in response to an absence of the GrIS, leading to a mean lower elevation of 1,340 m and altered land cover (i.e., growth of grass and shrubs). The bars represent the respective contributions in percentages, while the whiskers illustrate the 90 % confidence intervals. If not stated differently, values are computed from annual-mean values, except for the contributions to the changes in the storm tracks, which are calculated from DJF hourly data, and the mixed-layer depth, which is computed from annual-maximum values. The elevation contributions are computed as (noGrIS - CTRL) / (noGrIS_elev - CTRL) and the surface property contribution as (noGrIS - CTRL) / ((noGrIS - CTRL) - noGrIS_elev). Grey arrows show the direction of sea-ice transport and the blue arrows the direction of water-mass transport. The regions used to calculate the contributions are defined in the appendix A1. Gr = Greenland.

3.5 Impact of altered climatic conditions on the GrIS evolution

530 In the preceding sections, we demonstrated that a complete removal of the GrIS would significantly alter climate conditions in the Northern Hemisphere. As the climate feeds back onto the GrIS it would ultimately determine whether a new ice sheet may form. To investigate this matter, we ask the question: Could a new ice sheet form under the different climate conditions in

https://doi.org/10.5194/esd-2024-24
Preprint. Discussion started: 22 August 2024


Earth System Dynamics Discussions Open Access EGU

noGrIS? Answering this question is an important step towards a better understanding of a potential regrowth of the GrIS and its stability under altered climate conditions.

To address this question, we used hourly atmospheric input data of the last 100 years of each experiment (CTRL, noGrIS, noGrIS_elev) to calculate the surface mass balance (SMB), using an offline energy balance model (Kapsch et al., 2021). The energy balance model allows to calculate the SMB from the surface fluxes of the atmospheric model and to downscale it onto a high-resolution topography. Thereby, the SMB determines where snow can accumulate or melt, hence, gives an indication of whether the climate conditions are favorable for the formation and/or preservation of an ice sheet. To explore whether the CTRL or noGrIS climate conditions are more favorable for a potential regrowth of the GrIS, the SMB derived from CTRL was interpolated onto the PI ice-sheet (first column in Fig. 14) as well as on the noGrIS topography (referred to as CTRL_elev, second column in Fig. 14). Both topographies are shown in Fig. 1.

Accumulation

In CTRL, accumulation is highest in southern Greenland with a maximum along the coasts (Fig. 14a), aligned with the regions of maximum precipitation and high orography (Fig. 7a & 1a). In noGrIS, air masses can move further inland due to the lower topography (Sect. 3.1.2), leading to lower accumulation rates in western Greenland. The highest accumulation, although lower than in CTRL, occurs in the high-elevation parts of southeastern Greenland (Fig. 14c). noGrIS_elev shows that the orographic effect drives most of the redistribution (Fig. 14d), while GrIS surface properties play only a reinforcing role in the overall reduction in accumulation.

Ablation

In the cold CTRL climate, ablation is confined to the low-lying areas along the coast (Fig. 14e). Elevated temperatures in noGrIS enable widespread ablation across Greenland, with highest anomalies in regions characterized by a significantly lowered elevation (Fig. 14g). While in CTRL, ablation affects roughly 17 % of Greenland's land surface, in noGrIS, nearly the entire surface experiences melt. The expanded melt area, encompassing 97 % of Greenland's area in noGrIS, is primarily attributed to the reduced elevation (often referred to as melt-elevation effect (Vizcaino et al., 2015)) and associated with atmospheric circulation differences, evident in comparison with noGrIS_elev (Fig. 14h). The warming contribution from changed GrIS surface properties in noGrIS further increases the ablation rate.

Surface mass balance

With enhanced ablation and the redistribution of precipitation, a positive SMB, indicative of a net mass accumulation, only occurs within a restricted area of the eastern part of Greenland under the noGrIS climate (Fig. 14k). In this region, where surface elevation has decreased from approximately 2,400 to 1,300 m, elevated bedrock provides favourable conditions for ice-sheet nucleation. The sufficiently cold surface temperatures support year-round net accumulation in form of snow, sustaining a potential growth of an ice-sheet. Interpolating the SMB on the same topography as noGrIS shows that the CTRL climate would

https://doi.org/10.5194/esd-2024-24
Preprint. Discussion started: 22 August 2024


Earth System Dynamics Discussions
Open Access
EGU

promote the development of larger ice sheets, as the SMB is significantly larger along the South and East coast of Greenland as well as in small areas in the northwest of Greenland (Fig. 14j). This indicates that the differences in the background climate between CTRL and noGrIS can have a substantial impact on a potential regrowth of the GrIS (Sect. 3.1).

https://doi.org/10.5194/esd-2024-24
Preprint. Discussion started: 22 August 2024

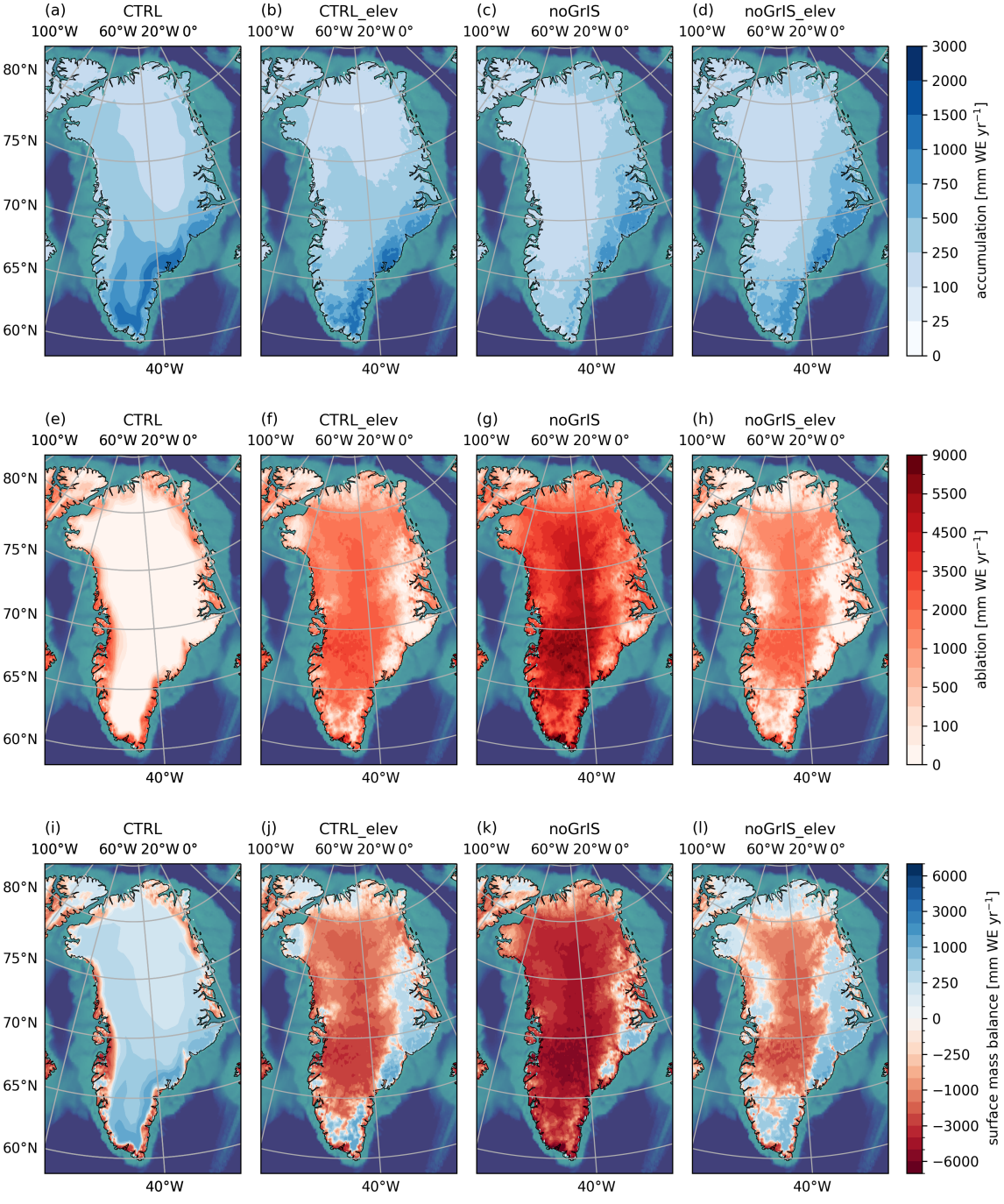

Figure 14. (a) Accumulation, (b) ablation and (c) SMB annually in Greenland. The first column shows the CTRL accumulation, ablation and SMB interpolated onto the PI topography. The second, third and fourth columns show the CTRL, noGrIS and noGrIS_elev accumulation, ablation and SMB, all interpolated on the noGrIS topography. Results are obtained from a SMB model forced offline with the climatology of the averaged output over the last 100 years of the three MPI-ESM simulations. Differences in the spatial details are due to the different resolutions of the underlying bedrock topographies with a, e and i being interpolated on a 10 min (about 18.5 km at the equator) grid and the remaining ones being interpolated onto a 10 km grid.

https://doi.org/10.5194/esd-2024-24
Preprint. Discussion started: 22 August 2024


Earth System Dynamics Discussions Open Access EGU

4 Discussion

Our use of a coupled atmosphere-ocean model with interactive vegetation and a sufficiently long model spin-up to reach equilibrium allowed to generate a systematic set of sensitivity experiments that enables us to comprehensively investigate the interactions of the GrIS with the full climate system, including the deep ocean. Hence, our study extends prior studies that employed either atmosphere-only (e.g., Dethloff et al., 2004; Hakuba et al., 2012; Junge et al., 2005; Petersen et al., 2004), simplified ocean models (e.g., Lunt et al., 2004), or coupled simulations yet to achieve full oceanic equilibrium (Davini et al., 2015; Stone and Lunt, 2013; Toniazzo et al., 2004). While these studies suppressed the ocean influence to the climate response to varying degrees, our study transcends by adding knowledge on the deep-ocean response. Through the variety of sensitivity studies, our research not only describes the changes but disentangles, attributes and quantifies the drivers of the ocean response.

For the atmospheric response, strong similarities to previous research findings exist. For example, the redistribution of precipitation, mainly as a consequence of the lower GrIS elevation as previously found (Stone and Lunt, 2013), emerges as a robust feature across various climate models (Davini et al., 2015; Dethloff et al., 2004; Lunt et al., 2004; Solgaard and Langen, 2012; Stone and Lunt, 2013; Toniazzo et al., 2004; Petersen et al., 2004). Further, the strongest warming in response to a removal of the GrIS occurs consistently over Greenland in all models (Crowley and Baum, 1995; Davini et al., 2015; Dethloff et al., 2004; Hakuba et al., 2012; Junge et al., 2005; Lunt et al., 2004; Ridley et al., 2005; Toniazzo et al., 2004; Vizcaíno et al., 2008), with a highest positive anomaly in summer attributed to the altered GrIS surface properties (Davini et al., 2015; Lunt et al., 2004; Ridley et al., 2005; Solgaard and Langen, 2012; Stone and Lunt, 2013; Toniazzo et al., 2004). While the largest climate responses broadly align between various studies, due to the dominance of the elevation effect, differences occur due to the utilized model systems (e.g., coupled atmosphere and ocean component) as well as the experimental setup (e.g., surface-albedo adjustments or isostatically adjusted vs. non-adjusted bedrock vs. surface elevation set to sea level). In winter, the lapse-rate effect dominates differences in temperatures over Greenland between noGrIS and CTRL, but our results also show that changes in the atmospheric circulation contribute to the winter temperature response. The latter supports findings by Stone and Lunt (2013) and Toniazzo et al. (2004) but is contrary to Lunt et al. (2004), who suggested that circulation changes are not decisive. We also find an increase in the cyclonic activity over Greenland, confirming previous findings by Vizcaíno et al. (2008), Hakuba et al. (2012) and Junge et al. (2005). Together with the altered temperature, the increased cyclonic activity over Greenland leads to the weakening of the Greenland Anticyclone and a deepening and expansion of the Icelandic Low (Toniazzo et al., 2004; Petersen et al., 2004; Davini et al., 2015). Cyclonic activity also increases to the east of Greenland, which is consistent with findings by Petersen et al. (2004) and Dethloff et al. (2004) but contrasts findings by Junge et al. (2005), Hakuba et al. (2012), Lunt et al. (2004) and Vizcaíno et al. (2008). This indicates that the local response is predominantly similar and robust against different model systems, whereas the distant response relies more on the type of coupling and/or the usage of simple methods for the adjustment of the GrIS orography and surface properties as well as on the resolution, as suggested previously by Junge et al. (2005).

In our simulations, the removal of the GrIS leads to an eastward shift of the 500 hPa quasi-static wave over Greenland. Further, we find that the shifted 500 hPa quasi-static wave plays a pivotal role in shaping the temperature response in our

https://doi.org/10.5194/esd-2024-24
Preprint. Discussion started: 22 August 2024


Earth System Dynamics Discussions Open Access EGU

simulations by intensifying the southerly wind component at 500 hPa over Greenland. The shift is accompanied by altered 10 m winds, resembling Toniazzo et al. (2004), which advect warm air from Greenland towards the Canadian Archipelago and the Labrador Sea. The change in winds results in a warming of the western Arctic. While this process is in line with Davini et al. (2015), it contrasts findings by Petersen et al. (2004) and Junge et al. (2005), who linked the warming to the west of Greenland to the reduced Greenland blocking, which allows for cold Arctic air that usually remains west of Greenland to disperse further eastward. However, their results were obtained with atmosphere-only models, unchanged GrIS surface properties and simple methods for the reduction of the GrIS elevation, neglecting important feedbacks between the ocean, topography and the orography. The shifted wave additionally induces an enhanced northerly inflow of cold polar air over the Barents Seas and Scandinavia, resulting in a local cooling, similar to Lunt et al. (2004). In contrast to Lunt et al. (2004), who found that the atmospheric change also leads to near-surface cooling that triggers sea-ice expansion in the Barents Sea, our sensitivity studies suggest that a stronger northerly component in the wind stress intensifies the southward drift of sea ice. The associated sea-ice expansion creates a negative feedback loop that further cools the overlying atmosphere. This mechanism contrasts with prior findings that associated parts of the cooling over the Barents Sea and neighboring land areas with reduced heat advection due to a decreased storm activity (south-)east of Greenland (Lunt et al., 2004; Ridley et al., 2005; Stone and Lunt, 2013; Toniazzo et al., 2004; Vizcaíno et al., 2008).

Davini et al. (2015) suggested a weakening of the AMOC associated with a reduced poleward Atlantic heat transport as an additional mechanism for the cooling over the North Atlantic and Eurasia. Their AMOC reduction is a consequence of reduced deep-water formation in the Nordic Seas and Labrador Sea. We also simulate reduced deep-water formation in the Nordic Seas, whereas the mixed-layer depth in the Labrador Sea increases. This can explain the difference in the AMOC response to an absent GrIS. In our simulations, the maximum AMOC strength as well as the Atlantic heat transport at the latitudes of Central Europe remain nearly unchanged, but the NADW cell is shallower. Our sensitivity experiments demonstrate that this cooling also prevails in simulations in which the AMOC experiences only a marginal weakening. Similar to our results, Toniazzo et al. (2004) also did not find a significant difference in the AMOC strength following a removal of the GrIS. This suggests that the contribution of the AMOC may be smaller than indicated in Davini et al. (2015) and that changes in the AMOC may not be the primary driver of the cooling over Eurasia and the Nordic Seas. Our analysis reveals a reduced heat loss of the Nordic Seas due to the larger sea-ice cover. The additional sea ice insulates the ocean and leads to a stronger ocean stratification that prevents the heat loss of the inflowing subsurface Atlantic waters. As a consequence, the water exported from the Nordic Seas through the Denmark Strait is warmer and contributes to the subsurface warming in the subpolar gyre. The cooling over the Nordic Seas emerges as a consequence of the combined effects of the altered atmospheric circulation and the expanded sea-ice cover that reduces heat loss towards the atmosphere. Over most of Scandinavia, the cooling is driven almost equally by atmospheric and oceanic feedbacks. South and east of Scandinavia the oceanic impact ceases.

Our study also shows that the disintegration of the GrIS has considerable implications for the ocean circulation and ocean properties in the Arctic. For example, our findings underscore the crucial role of changes in the wind stress on the upper ocean circulation, particularly the Nordic Seas, influencing the water-mass exchange with the Arctic Ocean, a finding which is in accordance with Davini et al. (2015). However, Davini et al. (2015) proposed that the GrIS elevation effect leads to the

https://doi.org/10.5194/esd-2024-24
Preprint. Discussion started: 22 August 2024

transport of fresher waters by the East Greenland Current along Cape Farewell toward the Labrador Sea. Consequently, this process freshens the Labrador Sea, lowers convection, and weakens the AMOC. While we also simulate fresher Nordic Seas, water in the Denmark Strait is fresher only until a depth of around 100 m but more saline and warmer in lower layers, due to the weaker (warmer and saltier) East Greenland Current. The anomaly extends across the Irminger Sea toward the Labrador Sea, where it contributes to the simulated warmer and more saline conditions. Although the increase in salinity, in the absence of the GrIS, leads to an increase in upper-ocean density in our study, deep convection does not increase enough to compensate for the reduced influx of overflow from the Denmark Strait. Hence, the NADW cell is shallower in noGrIS relative to CTRL. We also find that altered ocean dynamics in the western Arctic, regarded as negligibly influenced by the wind-stress changes in Davini et al. (2015), also contribute to the simulated changes in the Labrador Sea. The discrepancies between our study and Davini et al. (2015), specifically in the Labrador Sea, are likely related to differences in the model system and boundary conditions. Possible explanations include the usage of an isostatically-adjusted bedrock in our study compared to a non-adjusted bedrock in Davini et al. (2015), though Toniazzo et al. (2004) showed only minor differences in their impacts. Alternatively, the weak drift in the model of Davini et al. (2015) may cause different results. These discrepancies highlight the complex and regionally specific responses of the atmosphere and ocean to the absence of the GrIS, emphasizing the need for further research and model comparisons to fully grasp the broader implications of the presented climatic changes.

Our analysis of the consequences of removing the GrIS underscores the significant impact of the GrIS on atmosphere and ocean dynamics, altering the conditions conducive for a potential regrowth of the GrIS. Our simulations show that net snow accumulation would only be supported in areas of high-altitude bedrock in East Greenland in response to the altered climate conditions. This indicates that a return to a PI GrIS is unlikely under the changed climate. This is in line with Crowley and Baum (1995) and Toniazzo et al. (2004), who concluded that a meltdown of the GrIS would be irreversible under Holocene climate conditions, using snow accumulation as an indicator for ice-sheet regrowth in their General Circulation Models. One factor that leads to the irreversibly in our model is likely related to the lowering of the surface albedo, due to the growth of grass and shrubs, as suggested by Stone and Lunt (2013). However, as our model lacks two-way interactions between the ice sheet and the atmosphere and ocean, the climate change resulting from the formation of a small ice sheet could possibly favor an ice-sheet expansion. For example, Langen et al. (2012) showed that two-way coupling between the atmosphere and the ice-sheet is crucial for the development of an ice sheet. Nevertheless, previous simulations with an atmospheric General Circulation Model coupled to a dynamic ice-sheet model (Gregory et al., 2020) also showed that the GrIS does not fully regrow under PI climate conditions if its extent drops below a certain threshold. Similarly, using an AOGCM with dynamic vegetation coupled to an ice-sheet model, Vizcaíno et al. (2008) found that the ice sheet may maintain a bi-stability under PI CO_2 levels.

5 Conclusions

The experiments in this study simulate the climate following a complete disintegration of the GrIS. Employing a coupled atmosphere-ocean model, allowed us to provide a distinct attribution and quantification of the simulated global atmospheric and oceanic responses to their respective drivers. Our study unveils that the climatic response to a disintegrated GrIS is dominated

https://doi.org/10.5194/esd-2024-24
Preprint. Discussion started: 22 August 2024

by orographic effects and associated changes in the wind (stress), attributable to a reduced surface elevation of on average 1,320 m. Hence, the primary impact of the GrIS is induced by the ice sheet acting as a mechanical barrier. While this finding is consistent with previous research (e.g., Petersen et al., 2004), our study extends this understanding by revealing that altered GrIS surface properties amplify the majority of the climatic changes while they counteract some of them, for example, the change in ocean-mass transport through the Barents Sea Section and the Bering Strait. For the first time, an analysis reveals that the GrIS surface-property effect exerts a dominant influence in certain regions, notably pronounced in the Labrador Sea. We discern that the contribution of the effects varies not only horizontally but also vertically within the ocean. While changes in the elevation yield the greatest influence in the upper ocean layers, alterations in the surface properties emerge as an important driver of oceanic changes in the intermediate and deep layers. This distinction is unveiled only due to the use of a coupled model system including a fully spun-up deep ocean. Further, our analysis reveals a GrIS impact extending beyond the Northern Hemisphere (sub-)polar region, including a southward shift and shallowing of the North Atlantic subtropical gyre and a cooling of Central and Northern European 2 m air temperatures. Considering a potential disappearance of the GrIS under future global warming scenarios (Aschwanden et al., 2019), this would also result in significant socioeconomic consequences.

Using an offline energy balance model suggests that once disintegrated, a regrowth of the GrIS to PI extent would be inhibited, not only due to the lower GrIS surface elevation and associated lapse-rate effect but also because of changes in the background climate. This points towards a bi-stability of the GrIS, which is consistent with previous findings, and implies a potential irreversibility of present and future GrIS mass loss. However, the long-term climatic changes ultimately feed back onto the ice sheet, decisively determining its potential areas of regrowth. Future work will therefore use a comprehensive fully-coupled Earth System Model (ESM) encompassing dynamic ice sheets and vegetation to investigate whether a regrowth under the changed climate conditions would be possible. This will allow us to unravel so far neglected feedbacks between ice sheets and the climate system, while addressing the uncertainties that are associated with disregarding ice-sheet dynamics in simulations of the future climate with a comprehensive ESM.

Our analysis underscores the importance of taking into account all interactions and feedbacks between the GrIS and the full climate system when studying the future climate. To achieve this, it is not only imperative to allow for interactions between the different model components but also to consider long time scales of more than 5,000 years, allowing the deep ocean sufficient time to adjust to alterations in the Earth system. Our approach fills a critical gap, as the ocean response to a disintegrated GrIS had not previously been systematically linked to the surface-elevation and property effect, despite playing a substantial role in driving climate dynamics. This advances our understanding of the interplay of the GrIS with the full climate system, including the deep ocean.

Code and data availability. Model data and scripts used for the analysis are available through Zenodo (doi to follow) upon publication. The Max Planck Institute Earth System Model code is available upon request from the Max Planck Institute for Meteorology under the Software License Agreement version 2.

https://doi.org/10.5194/esd-2024-24
Preprint. Discussion started: 22 August 2024


Earth System Dynamics Discussions
Open Access
EGU

Appendix A: Regional means

Table A1. Regions used for the area means.

Variable	Coordinates
Mechanical blocking, annual warming, normalized 500-hPa geopotential height, weakened Greenland anticyclone, storm activity	Greenland
2 m temperature cooling over Central and Northern Europe	lon: 3.8 to 45.0° E lat: 46.4 to 68.7° N
10 m wind amplitude	lon: 11.25° W; lat: 79.78° N lon: 11.3° W; lat: 76.1° N lon: 11.3° W; lat: 72.4° N lon: 15.0° W; lat: 76.1° N lon: 15.0° W; lat: 72.4° N
Southward shift of the subtropical gyre: 10° C isotherme	lon: -66.4 to -18.9° E lat: 32.5 to 39.4° N
AMOC shallowing	lat: 40.0 to 60.0°
North Atlantic heat transport	lat: 50.0 to 80.0° N
Labrador Sea	
Mixed-layer depth	lon: -70.0 to -15.3° E lat: 42.1 to 62.5° N
Potential density (upper: 50-186 m / deep: 1888-2293 m), salinity, in situ temperature	lon : -47.2 to -42.0° E lat: 50.7 to 55.6° N
Nordic Seas	
Mixed-layer depth	lon: -20.2 to 27.7° E lat: 62.1 to 78.9° N
Potential density (upper: 50-186 m / deep: 1888-2293 m), salinity, in situ temperature	lon: -10.7 to 18.3° E lat: 63.8 to 75.7° N

https://doi.org/10.5194/esd-2024-24
Preprint. Discussion started: 22 August 2024


Earth System Dynamics Discussions Open Access EGU

Author contributions. All authors conceptualized the study and designed the experiments. MA carried out the simulations. MA performed the analysis and wrote the manuscript with input from all authors.

Competing interests. The authors declare that they have no conflict of interest.

Acknowledgements. MA was financially supported by the International Max Planck Research School on Earth System Modeling (IMPRS-ESM). MLK was funded by the German Federal Ministry of Education and Research as a Research for Sustainability Initiative through the PalMod project (grant no. 01LP2302A). All model simulations were performed at the German Climate Computing Center. The authors thank Chao Li for his critical feedback on a first version of the paper.

https://doi.org/10.5194/esd-2024-24
Preprint. Discussion started: 22 August 2024

Earth System Dynamics Discussions

References

Aschwanden, A., Fahnestock, M. A., Truffer, M., Brinkerhoff, D. J., Hock, R., Khroulev, C., Mottram, R., and Khan, S. A.: Contribution of the Greenland Ice Sheet to sea level over the next millennium, Science Advances, 5, eaav9396, 2019.

Berger, A. and Loutre, M. F.: Insolation values for the climate of the last 10 million years, Quaternary Science Reviews, 10, 297–317, 1991.

Box, J. E., Fettweis, X., Stroeve, J. C., Tedesco, M., Hall, D. K., and Steffen, K.: Greenland ice sheet albedo feedback: thermodynamics and atmospheric drivers, The Cryosphere, 6, 821–839, 2012.

Brovkin, V., Ganopolski, A., Archer, D., and Munhoven, G.: Glacial CO_2 cycle as a succession of key physical and biogeochemical processes, Clim. Past, 8, 251–264, 2012.

Crowley, T. J. and Baum, S. K.: Is the Greenland Ice Sheet bistable?, Paleoceanography, 10, 357–363, 1995.

Crowley, T. J., Yip, K.-J. J., and Baum, S. K.: Effect of altered Arctic sea ice and Greenland ice sheet cover on the climate of the GENESIS general circulation model, Global and Planetary Change, 9, 275–288, 1994.

Davini, P., von Hardenberg, J., Filippi, L., and Provenzale, A.: Impact of Greenland orography on the Atlantic Meridional Overturning Circulation, Geophysical Research Letters, 42, 871–879, 2015.

Dethloff, K., Dorn, W., Rinke, A., Fraedrich, K., Junge, M., Roeckner, E., Gayler, V., Cubasch, U., and Christensen, J. H.: The impact of Greenland's deglaciation on the Arctic circulation, Geophysical Research Letters, 31, 2004.

Gregory, J. M., George, S. E., and Smith, R. S.: Large and irreversible future decline of the Greenland ice sheet, The Cryosphere, 14, 4299–4322, 2020.

Hakuba, M. Z., Folini, D., Wild, M., and Schär, C.: Impact of Greenland's topographic height on precipitation and snow accumulation in idealized simulations, Journal of Geophysical Research: Atmospheres, 117, 2012.

Hobbs, W. W.: The Greenland glacial anticyclone, Journal of Atmospheric Sciences, 2, 143–153, 1945.

Jackson, L. C., Kahana, R., Graham, T., Ringer, M. A., Woollings, T., Mecking, J. V., and Wood, R. A.: Global and European climate impacts of a slowdown of the AMOC in a high resolution GCM, Climate Dynamics, 45, 3299–3316, 2015.

Junge, M. M., Blender, R., Fraedrich, K., Gayler, V., Luksch, U., and Lunkeit, F.: A world without Greenland: impacts on the Northern Hemisphere winter circulation in low- and high-resolution models, Climate Dynamics, 24, 297–307, 2005.

Kapsch, M. L., Mikolajewicz, U., Ziemen, F. A., Rodehacke, C. B., and Schannwell, C.: Analysis of the surface mass balance for deglacial climate simulations, The Cryosphere, 15, 1131–1156, 2021.

Kapsch, M.-L., Mikolajewicz, U., Ziemen, F., and Schannwell, C.: Ocean Response in Transient Simulations of the Last Deglaciation Dominated by Underlying Ice-Sheet Reconstruction and Method of Meltwater Distribution, Geophysical Research Letters, 49, e2021GL096 767, 2022.

Kleinen, T., Gromov, S., Steil, B., and Brovkin, V.: Atmospheric methane underestimated in future climate projections, Environmental Research Letters, 16, 094 006, 2021.

Köhler, P., Nehrbass-Ahles, C., Schmitt, J., Stocker, T. F., and Fischer, H.: A 156 kyr smoothed history of the atmospheric greenhouse gases CO2, CH4, and N2O and their radiative forcing, Earth Syst. Sci. Data, 9, 363–387, 2017.

Kristjánsson, J. E. and Mcinnes, H.: The impact of Greenland on cyclone evolution in the North Atlantic, Quarterly Journal of the Royal Meteorological Society, 125, 2819–2834, 1999.

Kristjánsson, J. E., Thorsteinsson, S., and Røsting, B.: Phase-locking of a rapidly developing extratropical cyclone by Greenland's orography, Quarterly Journal of the Royal Meteorological Society, 135, 1986–1998, 2009.

https://doi.org/10.5194/esd-2024-24
Preprint. Discussion started: 22 August 2024

Langen, P. L., Solgaard, A. M., and Hvidberg, C. S.: Self-inhibiting growth of the Greenland Ice Sheet, Geophysical Research Letters, 39, 2012.

Liu, W., Fedorov, A. V., Xie, S.-P., and Hu, S.: Climate impacts of a weakened Atlantic Meridional Overturning Circulation in a warming climate, Science Advances, 6, eaaz4876, 2024.

Lunt, D. J., de Noblet-Ducoudré, N., and Charbit, S.: Effects of a melted greenland ice sheet on climate, vegetation, and the cryosphere, Climate Dynamics, 23, 679–694, 2004.

Marsland, S. J., Haak, H., Jungclaus, J. H., Latif, M., and Röske, F.: The Max-Planck-Institute global ocean/sea ice model with orthogonal curvilinear coordinates, Ocean Modelling, 5, 91–127, 2003.

Mauritsen, T., Bader, J., Becker, T., Behrens, J., Bittner, M., Brokopf, R., Brovkin, V., Claussen, M., Crueger, T., Esch, M., Fast, I., Fiedler, S., Fläschner, D., Gayler, V., Giorgetta, M., Goll, D. S., Haak, H., Hagemann, S., Hedemann, C., Hohenegger, C., Ilyina, T., Jahns, T., Jimenéz-de-la Cuesta, D., Jungclaus, J., Kleinen, T., Kloster, S., Kracher, D., Kinne, S., Kleberg, D., Lasslop, G., Kornblueh, L., Marotzke, J., Matei, D., Meraner, K., Mikolajewicz, U., Modali, K., Möbis, B., Müller, W. A., Nabel, J. E. M. S., Nam, C. C. W., Notz, D., Nyawira, S.-S., Paulsen, H., Peters, K., Pincus, R., Pohlmann, H., Pongratz, J., Popp, M., Raddatz, T. J., Rast, S., Redler, R., Reick, C. H., Rohrschneider, T., Schemann, V., Schmidt, H., Schnur, R., Schulzweida, U., Six, K. D., Stein, L., Stemmler, I., Stevens, B., von Storch, J.-S., Tian, F., Voigt, A., Vrese, P., Wieners, K.-H., Wilkenskjeld, S., Winkler, A., and Roeckner, E.: Developments in the MPI-M Earth System Model version 1.2 (MPI-ESM1.2) and Its Response to Increasing CO2, Journal of Advances in Modeling Earth Systems, 11, 998–1038, 2019.

Meinshausen, M., Nicholls, Z. R. J., Lewis, J., Gidden, M. J., Vogel, E., Freund, M., Beyerle, U., Gessner, C., Nauels, A., Bauer, N., Canadell, J. G., Daniel, J. S., John, A., Krummel, P. B., Luderer, G., Meinshausen, N., Montzka, S. A., Rayner, P. J., Reimann, S., Smith, S. J., van den Berg, M., Velders, G. J. M., Vollmer, M. K., and Wang, R. H. J.: The shared socio-economic pathway (SSP) greenhouse gas concentrations and their extensions to 2500, Geosci. Model Dev., 13, 3571–3605, 2020.

Merz, N., Born, A., Raible, C. C., Fischer, H., and Stocker, T. F.: Dependence of Eemian Greenland temperature reconstructions on the ice sheet topography, Clim. Past, 10, 1221–1238, 2014a.

Merz, N., Gfeller, G., Born, A., Raible, C. C., Stocker, T. F., and Fischer, H.: Influence of ice sheet topography on Greenland precipitation during the Eemian interglacial, Journal of Geophysical Research: Atmospheres, 119, 10,749–10,768, 2014b.

Mikolajewicz, U., Gröger, M., Maier-Reimer, E., Schurgers, G., Vizcaíno, M., and Winguth, A. M. E.: Long-term effects of anthropogenic CO2 emissions simulated with a complex earth system model, Climate Dynamics, 28, 599–633, 2007.

Oerlemans, J. and Vugts, H. F.: A Meteorological Experiment in the Melting Zone of the Greenland Ice Sheet, Bulletin of the American Meteorological Society, 74, 355–366, 1993.

Ohmura, A. and Reeh, N.: New precipitation and accumulation maps for Greenland, Journal of Glaciology, 37, 140–148, 1991.

Peltier, W. R., Argus, D. F., and Drummond, R.: Space geodesy constrains ice age terminal deglaciation: The global ICE-6G_C (VM5a) model, Journal of Geophysical Research: Solid Earth, 120, 450–487, 2015.

Petersen, G. N., Kristjánsson, J. E., and Ólafsson, H.: Numerical simulations of Greenland's impact on the Northern Hemisphere winter circulation, Tellus A: Dynamic Meteorology and Oceanography, 56, 102–111, 2004.

Raddatz, T. J., Reick, C. H., Knorr, W., Kattge, J., Roeckner, E., Schnur, R., Schnitzler, K. G., Wetzel, P., and Jungclaus, J.: Will the tropical land biosphere dominate the climate–carbon cycle feedback during the twenty-first century?, Climate Dynamics, 29, 565–574, 2007.

Ridley, J. K., Huybrechts, P., Gregory, J. M., and Lowe, J. A.: Elimination of the Greenland Ice Sheet in a High CO2 Climate, Journal of Climate, 18, 3409–3427, 2005.

https://doi.org/10.5194/esd-2024-24
Preprint. Discussion started: 22 August 2024

Serreze, M. C., Carse, F., Barry, R. G., and Rogers, J. C.: Icelandic Low Cyclone Activity: Climatological Features, Linkages with the NAO, and Relationships with Recent Changes in the Northern Hemisphere Circulation, Journal of Climate, 10, 453–464, 1997.

Shepherd, A., Ivins, E., Rignot, E., Smith, B., van den Broeke, M., Velicogna, I., Whitehouse, P., Briggs, K., Joughin, I., Krinner, G., Nowicki, S., Payne, T., Scambos, T., Schlegel, N., A, G., Agosta, C., Ahlstrøm, A., Babonis, G., Barletta, V. R., Bjørk, A. A., Blazquez, A., Bonin, J., Colgan, W., Csatho, B., Cullather, R., Engdahl, M. E., Felikson, D., Fettweis, X., Forsberg, R., Hogg, A. E., Gallee, H., Gardner, A., Gilbert, L., Gourmelen, N., Groh, A., Gunter, B., Hanna, E., Harig, C., Helm, V., Horvath, A., Horwath, M., Khan, S., Kjeldsen, K. K., Konrad, H., Langen, P. L., Lecavalier, B., Loomis, B., Luthcke, S., McMillan, M., Melini, D., Mernild, S., Mohajerani, Y., Moore, P., Mottram, R., Mouginot, J., Moyano, G., Muir, A., Nagler, T., Nield, G., Nilsson, J., Noël, B., Otosaka, I., Pattle, M. E., Peltier, W. R., Pie, N., Rietbroek, R., Rott, H., Sandberg Sørensen, L., Sasgen, I., Save, H., Scheuchl, B., Schrama, E., Schröder, L., Seo, K.-W., Simonsen, S. B., Slater, T., Spada, G., Sutterley, T., Talpe, M., Tarasov, L., van de Berg, W. J., van der Wal, W., van Wessem, M., Vishwakarma, B. D., Wiese, D., Wilton, D., Wagner, T., Wouters, B., Wuite, J., and Team, T. I.: Mass balance of the Greenland Ice Sheet from 1992 to 2018, Nature, 579, 233–239, 2020.

Solgaard, A. M. and Langen, P. L.: Multistability of the Greenland ice sheet and the effects of an adaptive mass balance formulation, Climate Dynamics, 39, 1599–1612, 2012.

Stevens, B., Giorgetta, M., Esch, M., Mauritsen, T., Crueger, T., Rast, S., Salzmann, M., Schmidt, H., Bader, J., Block, K., Brokopf, R., Fast, I., Kinne, S., Kornblueh, L., Lohmann, U., Pincus, R., Reichler, T., and Roeckner, E.: Atmospheric component of the MPI-M Earth System Model: ECHAM6, Journal of Advances in Modeling Earth Systems, 5, 146–172, 2013.

Stone, E. J. and Lunt, D. J.: The role of vegetation feedbacks on Greenland glaciation, Climate Dynamics, 40, 2671–2686, 2013.

Toniazzo, T., Gregory, J. M., and Huybrechts, P.: Climatic Impact of a Greenland Deglaciation and Its Possible Irreversibility, Journal of Climate, 17, 21–33, 2004.

van den Broeke, M. R., Duynkerke, P. G., and Oerlemans, J.: The observed katabatic flow at the edge of the Greenland ice sheet during GIMEX-91, Global and Planetary Change, 9, 3–15, 1994.

Vizcaíno, M., Mikolajewicz, U., Gröger, M., Maier-Reimer, E., Schurgers, G., and Winguth, A. M. E.: Long-term ice sheet–climate interactions under anthropogenic greenhouse forcing simulated with a complex Earth System Model, Climate Dynamics, 31, 665–690, 2008.

Vizcaino, M., Mikolajewicz, U., Ziemen, F., Rodehacke, C. B., Greve, R., and van den Broeke, M. R.: Coupled simulations of Greenland Ice Sheet and climate change up to A.D. 2300, Geophysical Research Letters, 42, 3927–3935, 2015.

https://doi.org/10.5194/esd-2024-24
Preprint. Discussion started: 22 August 2024

Earth System Dynamics
Discussions
Open Access
EGU

Table 2. Water and sea-ice transport rates into the Arctic Ocean through the five Arctic straits connecting the Arctic Ocean and the surrounding oceans.

	Bering Strait		Canadian Archipelago		Nares Strait		Fram Strait		Barents Sea Section		Freshwater input
Experiments	Water	Sea ice	Water	Sea ice	Water	Sea ice	Water	Sea ice	Water	Sea ice	
CTRL	1.26	-0.0524	-0.52	-0.0002	-0.55	0.00236	-3.00	-0.0942	2.80	-0.0134	0.1479
noGrIS	1.21	-0.0653	-0.86	-0.0017	-1.01	-0.00410	-1.21	-0.0502	1.85	-0.0312	0.1478
noGrIS_elev	1.27	-0.0679	-0.79	-0.0009	-0.91	-0.00337	-1.31	-0.0612	1.74	-0.0327	0.1450
CTRL_wind	1.17	-0.0701	-0.91	-0.0009	-1.04	-0.00417	-1.15	-0.0471	1.93	-0.0385	0.1479